UNIVERSITY OF GHANA

COLLEGE OF BASIC AND APPLIED SCIENCES

INVESTIGATING CONDITIONS THAT MODULATE PYRAZINAMIDE SUSCEPTIBILITY IN *Mycobacterium tuberculosis*

RANEE AFLAKPUI

(10273372)

A THESIS SUBMITTED TO THE DEPARTMENT OF BIOCHEMISTRY, CELL AND MOLECULAR BIOLOGY, UNIVERSITY OF GHANA, IN PARTIAL FULFILMENT OF THE REQUIREMENTS FOR THE AWARD OF MASTER OF PHILOSOPHY DEGREE IN MOLECULAR CELL BIOLOGY OF INFECTIOUS DISEASES

JULY, 2017

DECLARATION

I, RANEE AFLAKPUI, declare that except for references to other people's work for which I have acknowledged, the experimental work described in this project was performed by me in the Microbiology and Immunology Department of the University of Minnesota Medical School, under the supervisions of Prof Anthony D. Baughn (Microbiology and Immunology Department of the University of Minnesota Medical School) and Dr. Lydia Mosi (Department of Biochemistry, Cell and Molecular Biology, University of Ghana.

…… Date: ……

RANEE AFLAKPUI

(Student)

…… Date: ……

PROF. ANTHONY D. BAUGHN

(Supervisor)

…… Date: ……

DR. LYDIA MOSI

(Supervisor)

ABSTRACT

Tuberculosis (TB) remains one of the major life threatening infectious diseases of public health concern globally. Its treatment is long and complex, requiring a cocktail of four drugs administered for six months. Pyrazinamide (PZA) is a cornerstone drug in the treatment regimen for tuberculosis that has contributed to reducing the treatment time from nine to six months. PZA is a pro-drug that is converted to its active form, pyrazinoic acid (POA) by the bacterial enzyme nicotinamidase. Unlike the other TB drugs, mechanistic basis for susceptibility and resistance to PZA are poorly understood. Recent studies have shown that PZA acts by depletion of thiol active coenzyme A (CoA) levels in *M. tuberculosis*. Using *M. bovis* BCG as a model organism, this study sought out to identify ways by which POA action can be potentiated, as well as identify novel POA resistance mechanisms. We also, tried to understand the mechanism by which host associated stresses potentiate PZA action. *Himar1* mariner-based transposon mutagenesis was conducted to identify novel POA resistance conferring mutations in BCG. Using checkerboard assays, we tested the hypothesis that oxidative stress potentiates POA action by oxidizing thiol active CoA thereby reducing its abundance. We also overexpressed phosphoenolpyruvate carboxykinase (*pckA*), a key player in CoA metabolism, to ascertain if this can enhance susceptibility to POA. From the transposon screen, it was identified that phage infection potentiates POA action by reducing the minimum inhibitory concentration of POA from approximately 2500 µg/ml to 75 µg/ml, possibly through induction of cell envelope stress. In addition, 62 POA resistant transposon mutants were isolated and 4 novel POA conferring mutations were identified. Synergy was observed between PZA and H_2O_2 resulting in enhanced susceptibility. POA conversion was also shown to be required for

this observed synergy with H_2O_2. Overexpression of *pckA* led to a 2-fold increased susceptibility of BCG to POA. We can conclude from this study that, host derived oxidative stress experienced by *M. tuberculosis* in macrophages, is potentially associated with POA action, and importantly, alterations in central carbon metabolism that modulate CoA abundance results in modulation of POA action.

DEDICATION

I dedicate this work to the Most High God for seeing me through the course of my Masters study. I also dedicate this work to my parents and family for being very supportive and loving.

ACKNOWLEDGEMENTS

I would like to express my sincerest appreciation to God for his grace, mercies, strength and protection throughout my Masters program. I also want to appreciate my supervisors Prof. Anthony D. Baughn and Dr. Lydia Mosi for their immense support, advice, suggestions and great mentorship. A very special thank you to Prof. Anthony Baughn for believing in me and allowing me to come perform my research in your laboratory. I remember how stressful the whole process was, but you always encouraged me. I am so grateful to you. I also wish to thank the members of Baughn laboratory as well as Tischler laboratory for their major inputs into my research, most especially, Dr. Anna Tischler, Joshua Thiede, Sarah Namugenyi and Alyssa Brokaw.

My greatest appreciation goes to West African Centre for Cell Biology of Infectious Pathogens (WACCBIP) for funding my tuition, research and supporting my upkeep with monthly stipends. My sincerest appreciation also goes to National Institute of Health and National Institute of Allergy and Infectious Diseases R01-AI123146 awarded to Prof. Anthony Baughn from which my research benefited immensely. I would also like to thank all my wonderful lecturers and the entire staff of the Department of Biochemistry, Cell and Molecular Biology of the University of Ghana and the Department of Microbiology and Immunology of the University of Minnesota for their vital role in my training.

Finally, I would love to appreciate my course mates for all their love, encouragement and support, most especially, Pheonah Badu, Ernestine Kubi and Elizabeth Laryea Akrong, for being more than sisters to me, and always giving me a shoulder to cry on. I love and appreciate you all.

TABLE OF CONTENTS

LIST OF FIGURES

LIST OF TABLES

LIST OF ABBREVIATIONS

AES	Allelic exchange substrate
ART	Anti-Retroviral Therapy
ATP	Adenosine triphosphate
BCG	Bacillus Calmette–Guérin
CCCP	Carbonyl cyanide 3-chlorophenylhydrazone
CCM	Central carbon metabolism
CDC	Center for Disease Control and Prevention
CoA	Coenzyme A
DOT	Directly Observed Therapy
EMB	Ethambutol
$FADH_2$	Reduced flavine adenine dinucleotide
FAS-I	Fatty acid synthetase I
FIC	Fractional inhibitory concentration
FICI	Fractional inhibitory concentration index
GFP	Green fluorescent protein
H_2O_2	Hydrogen peroxide
HIV	Human Immunodeficiency Virus
IFN-γ	Interferon gamma
IGRA	Interferon gamma release assay
IL	Interleukin
INH	Isoniazid
iNOS	Inducible nitric oxide synthase

MDR	Multi-Drug Resistance
MGIT	Mycobacterial growth indicator tube
MIC	Minimum inhibitory concentration
MTBC	*Mycobacterium tuberculosis* complex
NAD	Nicotinamide adenine dinucleotide
NADH	Reduced nicotinamide adenine dinucleotide
NADP	nicotinamide adenine dinucleotide phosphate
NOX	NADPH oxidase
PCR	Polymerase Chain Reaction
PEPCK	Phosphoenolpyruvate carboxykinase
POA	Pyrazinoic acid
PPD	Purified protein derivative
PPP	Pentose phosphate pathway
PRR	Pathogen recognition receptors
PZA	Pyrazinamide
qRT-PCR	Quantitative Reverse Transcription PCR
RIF	Rifampicin
RNS	Reactive nitrogen species
ROS	Reactive oxygen species
TB	Tuberculosis
TCA	Tricarboxylic acid
TDR	Totally-Drug Resistance
TLR	Toll-like receptors

TNF-α	Tumor necrosis factor alpha
WHO	World Health Organization
XDR	Extensively-Drug Resistance

CHAPTER ONE

1.0 INTRODUCTION

1.1 Background

Tuberculosis (TB), caused by the bacterium *Mycobacterium tuberculosis*, remains one of the biggest global public health concerns caused by an infectious agent. According to the 2017 report from World Health Organization (WHO), there were an estimated 10.4 million incident cases of tuberculosis in 2016, with an estimated 1.3 million TB deaths worldwide.

In Ghana, TB still poses a public health threat and the disease control is hampered by HIV co-infection, emergence of drug resistance, ineffective vaccine and low sensitive diagnostics (WHO, 2017). Although Ghana is not considered a high burden country for TB, a report by WHO in 2016 ranked Ghana as a high burden country (HBC) for TB/HIV co-infection. TB is reported among HIV patients, prisoners, miners, pregnant women and diabetic patients. In Ghana, TB is not restricted by geographical location. However, the variations in case notification observed in various regions is linked to better access to health facilities (NTP, 2015). It has been observed that, the prevalence of TB in Ghana increases with age, and the disease is predominant in adult males (WHO 2017).

The current recommended treatment regimen for tuberculosis is a short-course therapy of a cocktail comprising four first-line drugs; rifampicin (RIF), isoniazid (INH), pyrazinamide (PZA) and ethambutol (EMB). The treatment lasts for six months with all four drugs given for the first two months, followed by a four-month continuation phase of RIF and INH

(Lawn & Zumla, 2011).

Although the first line regimen has a high success rate, its future efficacy and therefore TB control worldwide is threatened by the emergence of drug resistant *M. tuberculosis* strains. Resistance can be to single or multiple drugs included in the treatment regimen. Multi-drug resistant TB (MDR-TB) is TB that is resistant to both rifampicin and isoniazid, the two most potent anti-TB drugs and it requires treatment with a second-line regimen. Extensively drug resistant TB (XDR-TB) is defined as MDR-TB which is also resistant to at least one drug in both of the two most important classes of medicines in an MDR-TB regimen, which are fluoroquinolones and second-line injectable agents which include amikacin, capreomycin or kanamycin (WHO, 2017). One strategy for reducing the burden of resistant TB would be to discover new drugs that could be used to target these strains. However, this takes time, as new drugs must go through numerous phases of testing before they reach the market. Other strategies would include improving the efficacy of anti-tubercular drugs that are already on the market and trying to understand the mechanisms by which *M. tuberculosis* becomes resistant to these drugs.

Pyrazinamide is a first line anti-tubercular drug which was introduced in tuberculosis treatment in the early 1950s. Addition of PZA, an analog of nicotinamide, to the combined anti-tuberculosis regimen reduced the length of the treatment from nine to six months (Steele & Des Prez, 1988), as well as reducing relapse rates (Somner, A. & Angel, 1981; Ormerod & Horsfield, 1987). PZA is a pro-drug which is passively diffused into the cytoplasm of the mycobacterium, where its efficacy relies on conversion to pyrazinoic acid

(POA); its active form. The bacterial enzyme pyrazinamidase or nicotinamidase is required for this conversion, and is encoded by the gene *pncA* (Scorpio & Zhang, 1996). Nicotinamidase is an enzyme which has a physiological role in the salvage pathway of biosynthesis of nicotinamide adenine dinucleotide (NAD), a vital compound in over 300 biochemical redox reactions (Foster & Moat, 1980).

PZA has been used clinically for more than 60 years, however, the mechanism behind its anti-mycobacterial action is still not known. Numerous models have been proposed for the mechanism of action of PZA, but the most widely accepted proposal is that active POA accumulates in the cytoplasm of the bacteria and is excreted from the bacilli by a weak efflux pump that has not yet been identified. Since the bacilli reside in acidic environments and the pKa of POA is 2.9, a fraction of extracellular POA can become protonated and subsequently reabsorbed into the bacterial cell. The inefficient efflux pump and accumulation of POA inside the bacteria results in disruption of mycobacterial membrane permeability and transport which subsequently leads to cellular damage (Zhang *et al.,* 1999). This model has however been challenged by Peterson *et al.,* (2015), who demonstrated that the susceptibility of *M. tuberculosis* to PZA and POA is not dependent on environmental pH and therefore cannot be attributed to cytoplasmic acidification and proton shuttling.

While effectiveness of PZA has been documented *in vivo* in guinea pigs (Dessau *et al.,* 1952), mice (Solotorovsky *et al.,* 1952), and humans (Yeager *et al.,* 1952), *in vitro* susceptibility to the drug wasn't seen until McDermott and Tompsett discovered that an

acidic growth medium is necessary for this observation (McDermott & Tompsett, 1954). Current literature classifies PZA as a bacteriostatic agent based upon its inability to kill *M. tuberculosis* cells during *in vitro* exposure. Pyrazinamide activity has also been shown to be abolished in immune compromised athymic nude mice (Almeida *et al.,* 2014). The conditional susceptibility of PZA *in vivo* therefore suggests a host derived component critical for its bactericidal activity.

Pyrazinamide has been suggested to disrupt bacterial central carbon metabolism. Recent studies have also shown that PZA acts by depletion of coenzyme A (CoA) levels in *M. tuberculosis* (Gopal *et al.,* 2016). Consistent with this observation, a study from our laboratory also showed depletion of CoA levels in the attenuated tuberculosis vaccine strain *M. bovis* BCG after treatment with POA (Rosen *et al.,* 2017).

Recently, two PZA resistant *M. tuberculosis* isolates from an 11-year-old HIV-negative male patient with caseous pneumonia and a 27-year old HIV-negative male patient with infiltrative tuberculosis were taken through whole genome sequencing. The sequencing revealed non-synonymous mutations in several protein coding genes including *aceE* (Maslov *et al.,* 2015). Using transposon mutagenesis, our laboratory also identified mutations in *aceE* and *pckA* in PZA resistant isolates (Unpublished data). The gene *aceE*, codes for the E1 component of the pyruvate dehydrogenase enzyme complex, an enzyme complex involved in the conversion of pyruvate to acetyl CoA in the glycolysis pathway. The gene *pckA* on the other hand, encodes phosphoenolpyruvate carboxykinase (PEPCK), an enzyme involved in the conversion of oxaloacetate to phosphoenolpyruvate in the

gluconeogenesis pathway (Sanwal, 1970).

1.2 Problem Statement

Tuberculosis is the major life threatening infectious disease ranked above human immunodeficiency virus (HIV). The highest burden of TB and TB related deaths occur in sub-Saharan Africa of which Ghana is a member country (WHO, 2016). The mechanisms of action for the other three drugs in the TB treatment regimen; INH, RIF and EMB are known. However, the mechanism of PZA action remains elusive. Currently, we do know how PZA is converted to its active form POA, but the mechanism by which POA elicits its bactericidal action is not known.

In addition, the contribution of PZA in the short-course tuberculosis drug regimen is also being defied by the spread of PZA resistant strains of *M. tuberculosis*. This situation is further exacerbated by the fact that the mechanism of resistance is poorly understood. Currently, the major mechanism of resistance to PZA according to most studies is the loss of pyrazinamidase activity due to mutations in *pncA* (Scorpio & Zhang, 1996). Loss of *pncA* function prevents the conversion of PZA to the active POA required for the drug's activity. *M. tuberculosis* can tolerate the loss of PncA, and absence in the NAD salvage pathway, due to its ability to synthesize NAD *de novo* (Begley *et al.*, 2001; Boshoff *et al.*, 2008). Mutation in *pncA* accounts for approximately two thirds of clinical cases (Scorpio & Zhang 1996; Scorpio *et al.*, 1997). However, some clinical isolates which maintain wild type *pncA* are still presumably resistant to PZA through unknown mechanisms. Although multiple models for PZA's mechanism of action and mechanism of resistance have been

previously proposed, they lack sufficient confirmatory evidence. It is therefore imperative to elucidate the mode of action of PZA as well as identify alternative mechanisms of PZA resistance.

1.3 Justification

This study was designed to enhance our understanding of the conditions that regulate PZA susceptibility in *M. tuberculosis*, and will thus aid in understanding the mechanism of action of this drug and mechanisms by which resistance to POA occurs. Determining the mode of action of PZA will aid in developing new compounds with similar activity which are capable of further shortening treatment duration but do not require conversion by the bacterial enzyme. Also, identifying the genetic basis for resistance will enable the development of rapid molecular-based diagnostics and provide possible insights into circumventing resistance.

1.4 Hypothesis

1. Maintaining a higher steady state level of CoA through disruption of *aceE* or *pckA* genes in *Mycobacterium tuberculosis* is responsible for the PZA resistance phenotypes of these strains.
2. PZA synergizes with host induced oxidative burst for the clearance of *Mycobacterium tuberculosis*.

1.5 Aim of Study

To investigate conditions that modulate pyrazinamide susceptibility in *Mycobacterium tuberculosis.*

1.6 Specific Objectives

Specifically, the study seeks to:

1. Perform *Himar1* mariner-based transposon mutagenesis to identify novel pyrazinoic acid (POA) resistance conferring mutations.
2. Perform checkerboard assays to test synergy between pyrazinamide (PZA) and hydrogen peroxide (H_2O_2).
3. Evaluate the role of *aceE* and *pckA* in pyrazinamide susceptibility by manipulating gene expression.
4. Compare susceptibility of mutant and wild type strains to pyrazinamide.

CHAPTER TWO

2.0 LITERATURE REVIEW

2.1 Global Burden of Tuberculosis

Tuberculosis (TB) is one of the major life threatening infectious diseases ranked above HIV. In 2016, an estimated 10.4 million new TB infections and 1.3 million TB deaths were reported. In addition, approximately 374,000 deaths also occurred among HIV/TB co-infected individuals. These figures are alarming and emphasize the burden of this disease even though the disease is curable with early detection and treatment. The disease is predominant in males than females with an estimated infection distribution of 6.7 million and 3.7 million respectively, representing a ratio of 1.8:1. Approximately 1.0 million children were also infected in 2016. Generally, variations in case fatality occurs across countries, and in 2016, this ranged from below 5% in a few countries to 20% mostly in the WHO African region. The high case fatality associated with TB especially in the WHO African region is because of under-diagnosis due to late reporting of cases, under-treatment, poor adherence to treatment regimen and HIV co-infection (WHO, 2017; Horne *et al*., 2010; Waitt & Squire, 2011).

2.2 The burden of Tuberculosis in Ghana

In Ghana, as in other sub-Saharan African countries, TB still remains a major public health problem. The disease prevalence increases with age, and it is predominant in adult males as shown in Figure 2.1 (WHO 2017).

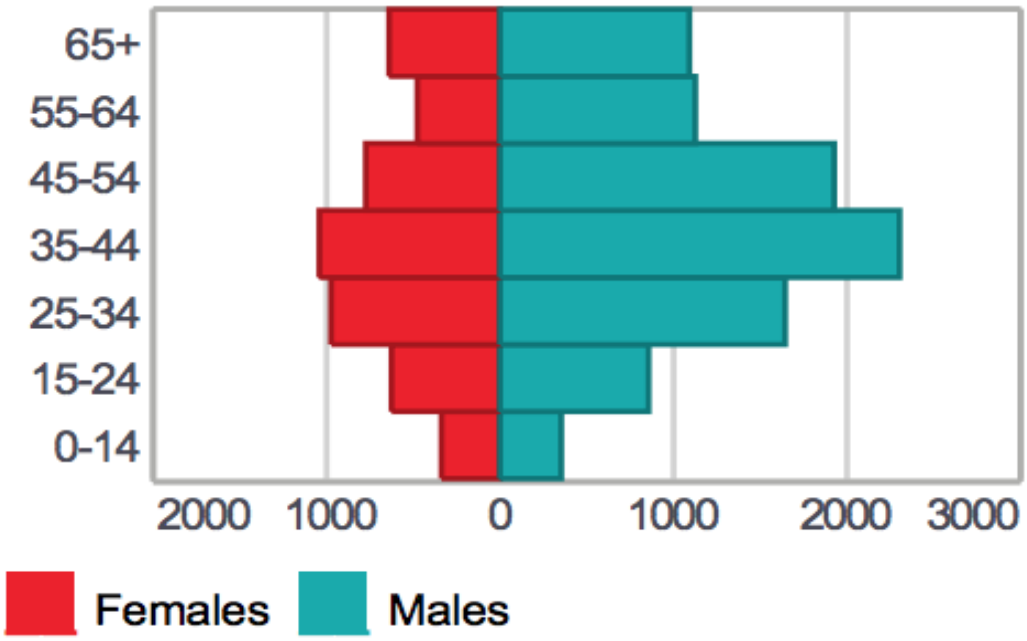

Figure 2.1: Tuberculosis case notifications in Ghana by age group and sex, 2016. (www.who.int/tb/data)

The disease brunt in Ghana was not acknowledged and promptly addressed as a public health emergency in the pre-independence era until in 1993 when the National Tuberculosis Control Programme (NTP) for Ghana was established with the aim to lead the fight against TB in the country (Amo-Adjei & Awusabo-Asare, 2013). In 1994, the NTP implemented the World Health Organisation's Directly Observed Treatment- Short course (WHO DOTS) Strategy. By the end of 1998, TB services had been integrated into primary health care, and DOTS coverage at the district level was estimated at 98% (GHS report, 2016).

In 2013, a national tuberculosis prevalence survey was conducted and the estimated TB prevalence was 290 per 100,000 population. This estimate when compared with the WHO

estimate for the same year (71 per 100,000 population) was 4 times higher in disease burden. This signified a low detection rate which was calculated as 20.7% based on the 2013 estimates (NTP, 2013). The very low cases seen at health institutions compared to the actual burden could be attributed to the stigmatization associated with the disease. For instance, TB is known among the people of the Volta region of Ghana as '*yomokpe*', meaning 'graveyard'. It is believed that once an individual is infected, death is inevitable. As a result, most TB-infected persons rather resort to spiritual healing than to show up at hospitals to get proper treatment (Lawn, 2000).

In 2016, WHO reported Ghana as a high burden country for TB/HIV. The TB incidence rate as reported by the WHO in 2016 was 156 per 100,000 population. Also, the estimated Multi-drug Resistant TB (MDR-TB) incidence reported in 2016 was 3 per 100,000 population (WHO, 2017). Until recently, Extensive or Extreme Drug Resistant TB (XDR-TB) was thought to be absent in Ghana but work done by Osei-Wusu *et al.,* 2018 has confirmed one case in the country.

2.3 Transmission of Tuberculosis

TB is caused by the bacterium *Mycobacterium tuberculosis*. Transmission of TB is exclusively through inhalation of aerosols containing the tubercle bacilli called droplet nuclei. This is produced by an individual with active disease through coughing, sneezing, talking and singing (Todar, 2008; Knechel, 2009). Factors that influence TB transmission include; enclosed environments with limited sunlight and poor ventilation, the number of bacilli present in the droplet nuclei, virulence of the organism and susceptibility (or

immune status) of an exposed host (Escombe *et al.*, 2007; CDC, 2005). The number of bacilli usually associated with infection ranges from 1-200 bacilli but, a droplet nuclei can contain up to 400 bacilli (Mayer 2010). Once inhaled, these bacilli move through various organs and finally settle in the alveoli (CDC, 2005). This could result in outright elimination of bacilli by muco-ciliary or innate immune mechanisms or establishment of TB infection in the lungs (which occurs 95% of the time) (Schluger, 2005). However, the TB infection may occur as an active disease or latent infection. It has been established that, about 5%-10% of TB infections develop into active disease within the first 5 years after exposure (Milburn, 2007) whereas, 5%-10% of infected persons also develop active disease at a much advanced stage in life (Batra, 2011; Telles & Kritski, 2007). Disseminated TB infection also occurs especially in immunosuppressed individuals like HIV patients through lymphatic or hematogenous spread of the bacilli.

2.4 Pathogenesis of Tuberculosis

The tubercle bacilli in the droplet nuclei that evade muco-ciliary expulsion and reach the alveoli trigger innate immune response mediated by host alveolar macrophages. These bacilli are mostly recognized by macrophages through interaction of pathogen recognition receptors (PRR) like the Toll-Like receptor-2 (TLR2) of macrophages (Nicod, 2007) with pathogen associated molecules, for example, surface carbohydrates, lipoproteins or peptidoglycans. The complement system also enhances pathogen recognition of macrophages and results in phagocytosis.

After internalization, proteolytic enzymes and cytokines such as interleukin (IL-1 and IL-12) and tumour necrosis factor alpha (TNF-α) are produced by the macrophages to degrade the pathogen and amplify the immune response, respectively (Van Crevel *et al*., 2002; Nicod, 2007). However, *M. tuberculosis* usually persists in macrophage due to its cell wall and secreted factors which prevent the fusion of phagosome and lysosome, thus, evading the killing mechanisms of the phagolysosome (Keane *et al.,* 1997). Some of the killing mechanisms of the phagolysosome are the generation of reactive oxygen and nitrogen species. Consequently, the bacilli still proliferate within the alveolar macrophages (Porth, 2002; ATC & CDC, 2000), and stimulate the production of pro-inflammatory cytokines which recruits leukocytes such as neutrophils, monocytes, dendritic cells and T-cells to the site. These immune effectors accumulate and are organized into a structure called granuloma (Takeda & Akira, 2005), also stabilized by chemokines such as CCL2, CCL3, CCL5, CXCL8, and CXCL10 (Saunders & Britton, 2007). The formation of the granuloma together with the constant cellular activation limits *M. tuberculosis* replication and spread leading to the development of a localized infection termed latent TB. This necrotic environment created is characterized by low oxygen, pH and nutrient levels (Ahmad, 2011; Cardona, 2009; Dheda *et al.,* 2005).

In immune competent individuals, the granuloma formed is calcified and so the infection is well contained. However, in immune-compromised individuals, although the granuloma formation is initiated, the immune deficiency and deregulation makes it unsuccessful with associated loss of integrity of the calcified structure. The bacilli therefore spread to other

parts of the lungs resulting in active disease (Van Crevel *et al*., 2002; Dheda *et al*., 2005). This process is summarized in Figure 2.2.

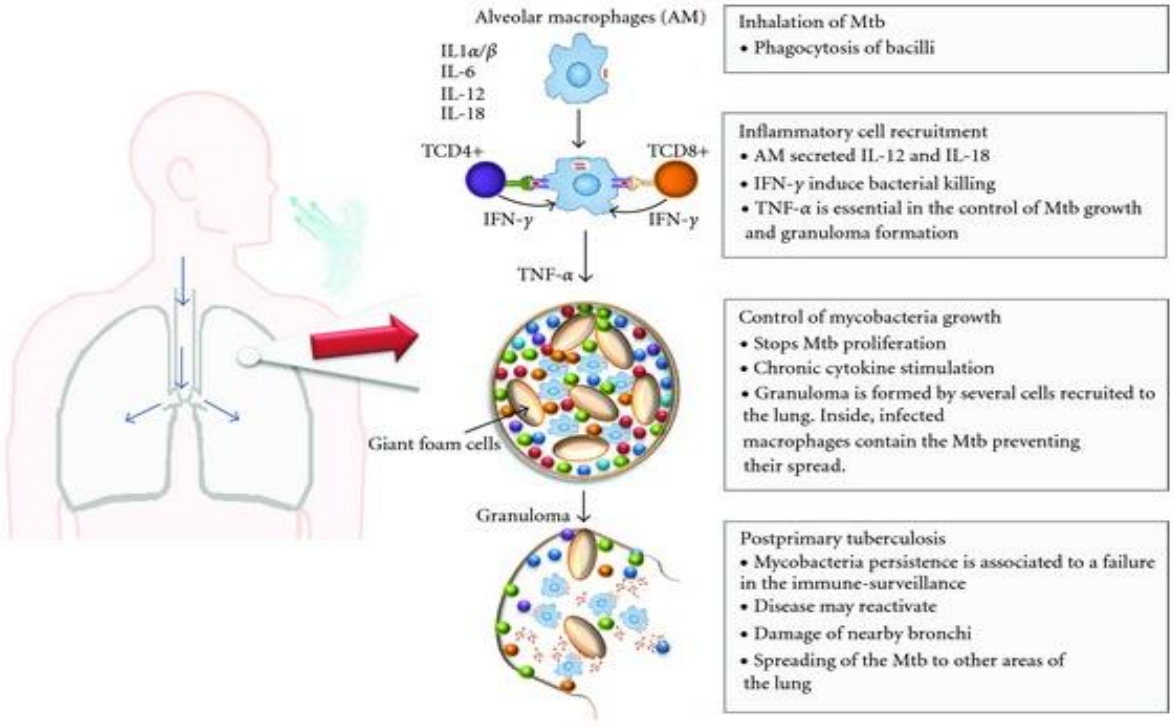

Figure 2.2: Pathogenesis of tuberculosis (Zuniga *et al.*, 2012).

2.5 Intracellular Environment Occupied by *M. tuberculosis* in the Host

The production of reactive oxygen species (ROS) and reactive nitrogen species (RNS) by human alveolar macrophages plays a principal role in controlling an *M. tuberculosis* infection. Phagocytes such as macrophages generate superoxide (O_2^-) in the phagosome by the NADPH oxidase multi-subunit complex (NOX2) through the transfer of electrons to molecular oxygen. Once produced, O_2^- can dismutate to a stable form; hydrogen peroxide (H_2O_2). The H_2O_2 can further react with O_2^- and metal ions to produce hydroxyl radicals (Minakami & Sumimotoa, 2006). These highly reactive and toxic species result in effective killing of the bacteria.

Likewise, reactive nitrogen species (RNS), are also very key antimicrobial effectors dominant in phagocytic cells. Nitric oxide (NO) is the primary form of RNS produced, and it is generated by the inducible nitric oxide synthase (iNOS) through a 2-step reaction that results in the production of NO and citrulline through the oxidation of L-arginine (Mayer & Hemmens, 1997). The production of RNS is induced by pro-inflammatory cytokines such as TNF, interleukins and interferon gamma (IFN-γ) in response to an infection (Fang, 2004). Together, ROS and RNS act synergistically by exerting extremely toxic effects on the invading microbes, leading to impaired metabolism, irreparable DNA damage and eventually results in killing of the bacteria.

2.6 Signs and Symptoms of Tuberculosis

Tuberculosis which affects the lungs is the most common type of TB although extra-pulmonary disease which can affect any part of the body also occurs. The commonest sign of pulmonary TB is cough that lasts beyond 2 weeks and may be non-productive at the initial stage but becomes productive with muco-purulent sputum as tissue necrosis and inflammation increase (Wani, 2013). Other clinical presentations of TB include; breathlessness, chest pain, weight loss associated with anorexia, fever, haemoptysis (sputum with streaks of blood), night sweats, wasting and terminal cachexia (Dormandy, 1999; WHO, 2015). Extrapulmonary TB is characterized by non-specific clinical presentation and the symptoms include those of pulmonary disease in addition to hepatomegaly, splenomegaly and lymphoadenopathy (Wani, 2013).

2.7 Diagnosis of Tuberculosis

Active TB is diagnosed by identification of acid fast bacilli in sputum cultures of suspected patients by smear microscopy, after Zeihl-Neelsen staining, culture and immunological tests. A chest x-ray is also a typical part of initial diagnosis (Konstantinos, 2010). Recently, rapid and more sensitive tests for TB and drug resistant TB based on molecular methods have been developed. These methods include GeneXpert MTB/RIF (Cepheid International, 2011) and line probe assays (LPAs). The GeneXpert MTB/RIF is a cartridge based, automated assay that is designed to detect Mycobacterium Tuberculosis Complex (MTBC) and rifampicin resistance. This assay functions by detecting the MTBC specific RNA polymerase DNA and the known mutations at the 81base pair hotspot region of rpoβ using real time PCR. This assay is rapid and has a relatively short turnaround time of around 2 hours. It also requires low infrastructure demand, hence can be used at the point of care. However, it is relatively expensive (Boehme, 2010; Cepheid International, 2011). Latent TB on the other hand, is diagnosed by the Mantoux tuberculin skin test, also referred to as the purified protein derivative test (PPD test) (Escalante, 2009). This test requires the intradermal injection of bacterial protein derivatives into the skin. When a person has been exposed to the bacteria, an immune response is expected to be mounted in the skin, resulting in an induration which can be measured. Interferon gamma (IFN-γ) release assays (IGRA), on a blood sample, is also used for diagnosing TB (Metcalfe *et al.*, 2011). This test relies on the fact that IFN-γ will be released by T-lymphocytes when exposed to specific antigens. The currently available IFN-γ release assays for diagnosis of TB are QuantiFERON-TB Gold and T-SPOT.TB.

2.8 Treatment of Tuberculosis

TB treatment involves taking multiple drugs for 6-24 months. The standard treatment regimen recommended by the WHO and Center for Disease Control and Prevention (CDC) comprises an intensive phase of 2 months administration of the first line anti-TB drugs; rifampicin (RIF), isoniazid (INH), pyrazinamide (PZA) and ethambutol (EMB). This is followed by a 4 month continuation phase of RIF and INH. Administration of daily doses of these drugs under close monitoring termed Directly Observed Therapy (DOT) is preferred to intermittent dosing (CDC, 2016; WHO, 2016). The continuation phase therapy can sometimes extend to 7 months. Such instances occur in patients with cavitary pulmonary TB caused by drug sensitive strains whose culture is positive after the 2 month intensive phase, patients whose regimen excludes PZA, and HIV/TB co-infected persons not on anti-retroviral therapy (ART) during TB treatment (CDC, 2016). Treatment is successful when a patient's sputum smear result is converted from positive to negative after 6 months of treatment. In the case where smear result remains positive after the 6 month period of therapy, treatment failure is said to occur (WHO, 2010).

Due to the thick hydrophobic cell wall and slow growing nature of *M. tuberculosis*, the anti-mycobacterial drugs in the treatment therapy acts by targeting multiple essential mycobacterial functions.

Isoniazid is a pro-drug that is activated by mycobacteria's catalase-peroxidase enzyme encoded by the gene *katG* (Zhang *et al*., 1992). The activated isoniazid produces reactive species which react with nicotinamide adenine dinucleotide (NAD+) and nicotinamide adenine dinucleotide phosphate (NADP+) to inhibit mycobacterial metabolic enzymes

such as the NADH-dependent enoyl-ACP reductase, encoded by *inhA* gene. This eventually results in the inhibition of mycolic acid synthesis in the bacterial cell wall, depletion of nucleic acid and killing of the bacteria (Timmins & Deretic, 2006). Rifampicin also acts by binding and inhibiting bacterial DNA dependent RNA polymerase, hence inhibiting transcription (Campbell & Korzheva, 2001). Ethambutol acts by disrupting the formation of mycolyl-arabinogalactan-peptidoglycan complex in the bacterial cell wall. Ethambutol interrupts the formation of arabinogalactan by targeting arabinosyl transferase, an enzyme required for the synthesis of this polysaccharide (Telenti *et al.,* 1997). The prolonged treatment duration is also necessary to completely kill all bacteria including persisters (bacteria in a state of dormancy which renders them resistant to otherwise bactericidal antibiotics) (Connolly *et al.,* 2007).

In addition to the anti-TB drugs, there is currently only one vaccine available for TB, called Bacillus Calmette–Guérin (BCG) and a dose is administered to healthy babies after birth. BCG provides protection in infants and young children. However, this protection wanes and normally lasts between ten and twenty years (WHO, 2004).

2.9 Drug Resistance in *M. tuberculosis*

Compounding the TB problem is the emergence of drug resistant strains of *M. tuberculosis*. Drug resistance occurs when the type of *M. tuberculosis* a patient is infected with is able to tolerate clinically achievable concentrations of at least one of the main TB drugs (Muller *et al.,* 2013). Drug resistance can occur as a result of wrong treatment regimen or failure of the patient to comply with treatment. There are also cases where a new patient can

directly be infected with a resistant TB bacilli. This is termed primary resistance (Fisher & Mobashery, 2010). The most alarming issue driving the global TB epidemics is the emergence of multi-drug resistance tuberculosis (MDR-TB). In 2016, there were 490 000 million cases of MDR-TB and about 200,000 deaths from MDR-TB. There were also an additional 110 000 cases that were susceptible to isoniazid but resistant to rifampicin. Furthermore, extensively drug resistance tuberculosis (XDR-TB) was reported in 91 countries and the average proportion of MDR-TB cases with XDR-TB was 6.2% (WHO, 2017). Lately, totally drug resistant (TDR) isolates have also been reported in Italy, Iran and India (Migliori *et al.,* 2007; Velayati *et al.,* 2009; Udwadia *et al.,* 2011).

Drug resistant *M. tuberculosis* infections are associated with increased treatment duration, leading to increased patient non-compliance on the recommended treatment regimen (Iseman, 2002), further promoting development of resistance. Additionally, drug resistant infections result in an increased mortality rate. For example, MDR and XDR infections have a high mortality rate at 40% and 60% respectfully. In 2016, there were about 240,000 deaths from MDR/Rifampicin resistant TB. Moreover, based on historical data, untreated *M. tuberculosis* infections are associated with an approximate 70% mortality rate (WHO, 2017; Tiemersma *et al.*, 2011).

As reported by WHO in 2016, new cases of MDR-TB and RIF-resistant TB cases estimated by the end of 2016 was 490,000 and 110,000 respectively (WHO, 2016). Drug resistance renders an otherwise treatable disease difficult to treat as shown by recent data on treatment. The treatment success rate for TB, MDR- TB and XDR-TB were 83%, 52% and

28% respectively. Global efforts geared towards overcoming the drug resistance challenge include strict monitoring of treatment to ensure patient compliance with treatment regimen and the introduction of bedaquiline in 70 countries and delamanid in 39 countries in 2015 for treatment of XDR TB (WHO, 2017; Lachâtre *et al*., 2016).

2.10 Central Carbon Metabolism in *M. tuberculosis*

Central carbon metabolism (CCM) is defined as the enzyme catalyzed transformation of carbon through glycolysis, gluconeogenesis, tricarboxylic acid (TCA) cycle, the pentose phosphate pathway (PPP), glyoxylate shunt, and methylcitrate cycle into products which are required for energy generation, metabolism and general physiology of an organism. Glycolysis is a metabolic pathway that converts glucose to pyruvate and then ultimately releases free energy which forms the high-energy ATP (adenosine triphosphate) and NADH (reduced nicotinamide adenine dinucleotide), (Baughn and Rhee, 2014).

The tricarboxylic acid (TCA) cycle, also known as Krebs cycle is a series of chemical reactions employed by all aerobic organisms to generate energy through the oxidation of acetyl-CoA into chemical energy in the form of ATP and produces carbon dioxide as a waste by product. TCA cycle also generates reducing equivalents, normally in the form of NAD(P)H and $FADH_2$ which can then participate in various oxido-reductive processes throughout central metabolism. Beyond these roles, it is also critical for providing essential substrates for biosynthesis of many amino acids, cofactors, and nucleotides (Baughn and Rhee, 2014).

Gluconeogenesis is a metabolic pathway used to generate glucose from certain non-carbohydrate carbon substrates such as lipids and proteins. Glucose can also be generated from other products of metabolism including pyruvate and lactate. The pentose phosphate pathway (PPP) is a metabolic pathway similar to glycolysis. It involves oxidation of glucose to generate mostly 5 carbon sugars as well as as ribose 5-phosphate, which is used in the synthesis of nucleotides. The glyoxylate shunt, a variation of the TCA cycle, mainly acts by converting acetyl-CoA to succinate which is used to synthesize carbohydrates (Kondrashov *et al.*, 2006). The glyoxylate shunt is very important in microorganisms since it allows the cells to exploit the use of simple carbon compounds as a carbon source in the absence of complex sources such as glucose (Lorenz *et al.,* 2002). The CCM of *M. tuberculosis* is shown in Figure 2.3.

M. tuberculosis' CCM has been shown to play a very vital role in not just physiology, but also in its pathogenesis (Sassetti *et al.,* 2003). Mutation studies identified genes whose disruption led to profound attenuations of *M. tuberculosis*. Isocitrate lyase (*Icl*), encoded by *Icl1*and *Icl2* is required for *M. tuberculosis*' to persist and survive in macrophages as well as in mice (McKinney *et al.,* 2000). *Icl* is an enzyme in the glyoxylate shunt that is responsible for catalyzing the cleavage of isocitrate to succinate and glyoxylate. Glyoxylate then condenses with acetyl-CoA, catalyzed by malate synthase, to form malate (Tanaka *et al.*, 1990).

Dihydrolipoyl transacetylase (*dlaT*), has also been shown to be crucial in the growth and pathogenesis of *M. tuberculosis.* Dihydrolipoyl transacetylase is the E2 component of the

pyruvate dehydrogenase complex, which is involved in the pyruvate decarboxylation reaction that links glycolysis to the citric acid cycle. A study by Shi and Ehrt in 2006, observed *in vitro* a retarded growth in an H37Rv knockout strain of *dlaT* (H37Rv*ΔdlaT).* This mutant strain was also readily killed by mouse macrophages. This study also showed that *dlaT* was required for full virulence in mice. Other CCM genes whose disruption have *led* to profound attenuations of *M. tuberculosis* include *pckA,* encoding phosphoenolpyruvate carboxykinase (PEPCK), involved in gluconeogenesis (Sassetti *et al.*, 2003), as well as *lpd*, which encodes lipoamide dehydrogenase, the third enzyme in pyruvate dehydrogenase complex (Venugopal *et al.*, 2011).

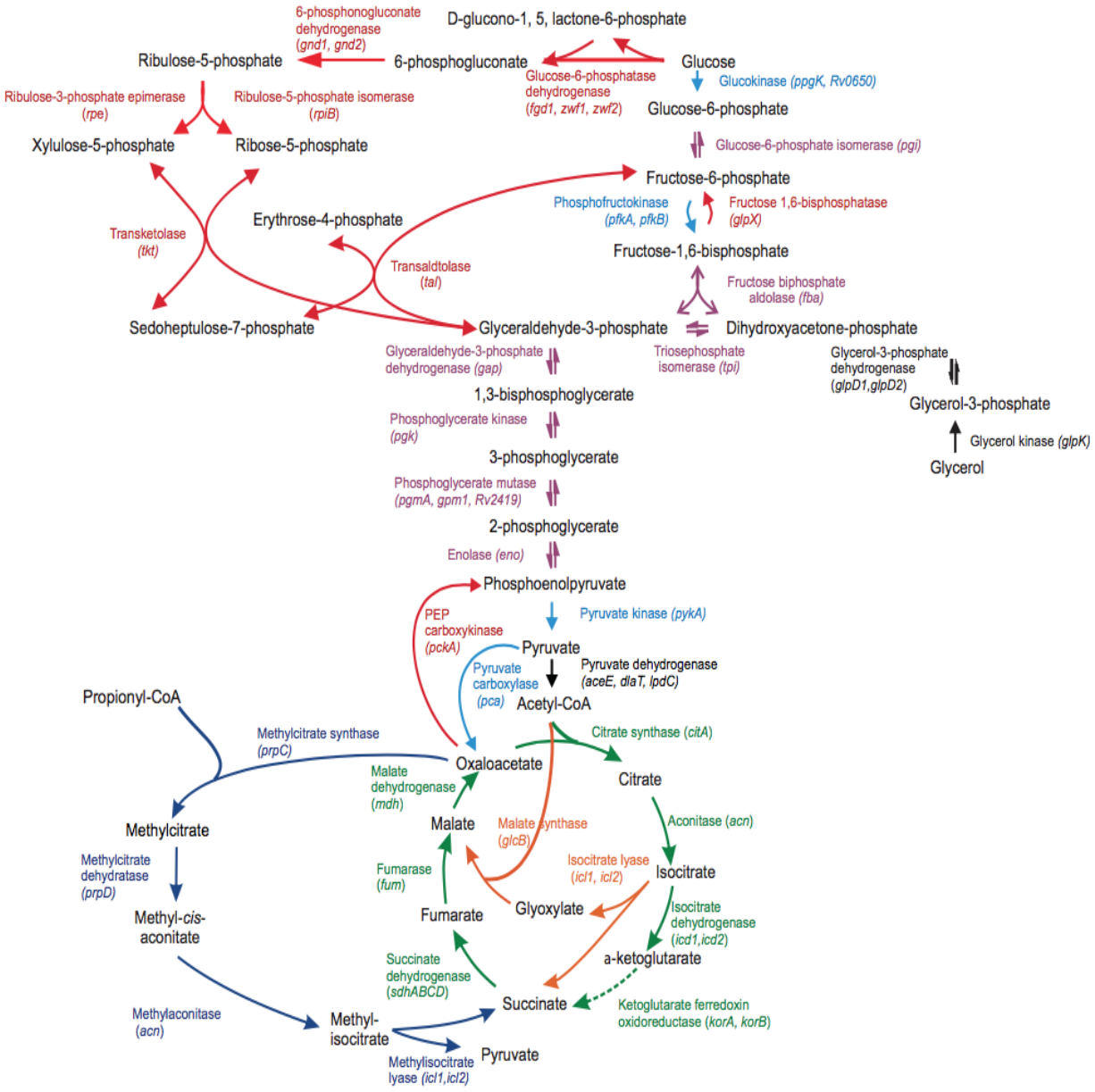

Figure 2.3: The schematic representation of the central carbon metabolism network of *M. tuberculosis*. Purple arrows represent reversible steps of glycolysis/gluconeogenesis, light blue: dedicated steps of glycolysis, pink: dedicated steps of gluconeogenesis, red: PPP, green: the TCA cycle, orange: the glyoxylate shunt, and dark blue: the methylcitrate cycle. The dotted green line indicates a standing question of connectivity in the TCA cycle via ketoglutarate ferredoxin oxidoreductase. Common enzyme names are shown next to the reactions they catalyze. Gene symbols are shown in parentheses. (Baughn and Rhee, 2014).

2.11 Pyrazinamide

The discovery of pyrazinamide (PZA) was a serendipitous one. In 1945, Ernst Huant attempted the use of nicotinamide to treat patients undergoing radiation therapy for lung tumors. Nicotinamide, a structural analog of PZA (Figure 2.4), was administered in the hope of protecting the lung mucosal layers from the detrimental effects of radiation. Although he did not observe the desired mucosal protection he anticipated, he did find that patients with TB associated lesions had reduced lesions after administration of this compound. This led him to conclude that nicotinamide had potential as an anti-mycobacterial drug (Huant, 1945). Subsequently, screens were conducted by multiple groups to identify structural analogs of nicotinamide which had improved anti-mycobacterial activity (Kushner *et al.,* 1952). Out of these screens came both isoniazid (Bernstein *et al.,* 1952) and pyrazinamide (Malone *et al.,* 1952) in 1952. Pyrazinamide is a very important component of the first line therapy to treat *M. tuberculosis* infections due to its combinatorial role in reducing treatment duration from nine to six months, while decreasing disease relapse rates (Somner, A. & Angel, 1981; Ormerod & Horsfield, 1987).

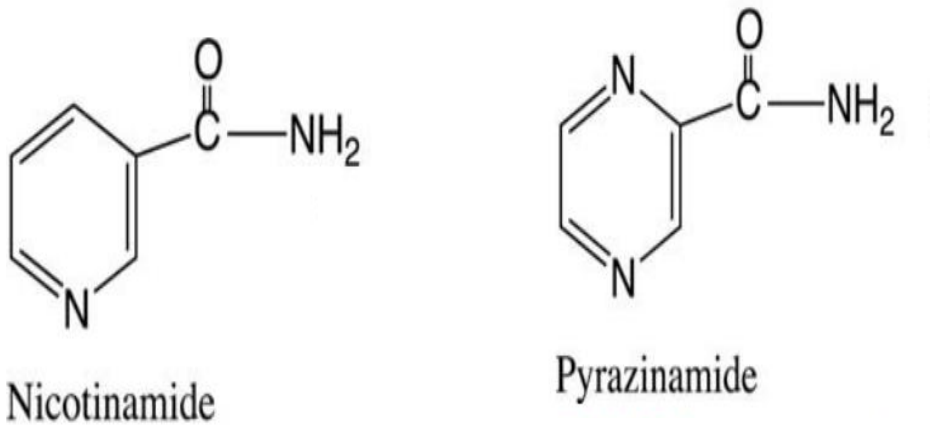

Figure 2.4: Nicotinamide and its structural analog pyrazinamide

Pyrazinamide is a prodrug whose efficacy requires that the drug is converted into the activated form pyrazinoic acid (POA). Formation of POA occurs through the hydrolysis of PZA by the mycobacterial pyrazinamidase/nicotinamidase, encoded by *pncA.* PncA is involved in the nicotinamide adenine dinucleotide salvage pathway in *M. tuberculosis* through the hydrolysis of nicotinamide to form nicotinic acid and ammonia (Figure 2.5).

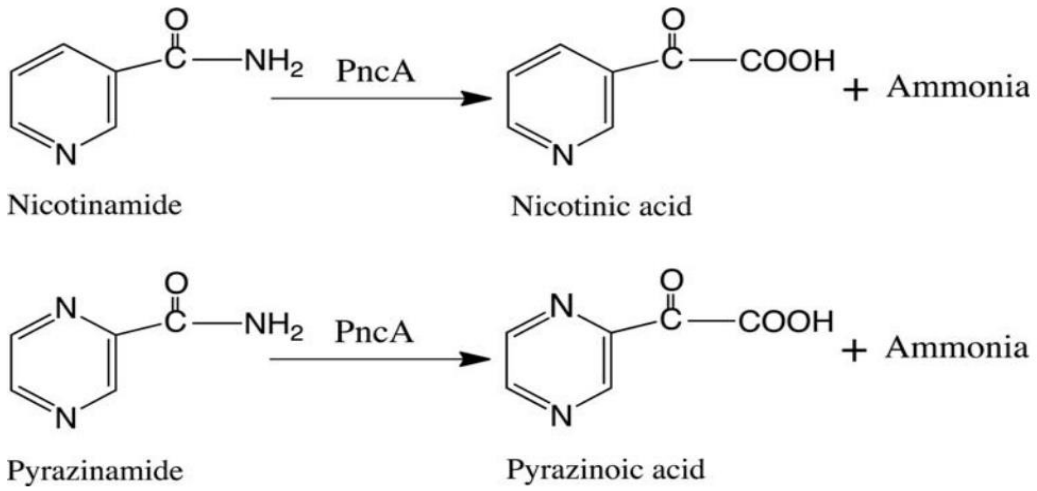

Figure 2.5: Conversion of nicotinamide and PZA to nicotinic acid and POA, respectively, by pyrazinamidase/nicotinamidase, encoded by the *pncA*.

2.12 Factors That Affect PZA Action

PZA is very different from common antibiotics. This is because, while common antibiotics are basically active against replicating bacteria and have minimal or no activity against non-replicating bacteria, PZA is mainly active against non-growing persisters (Zhang *et al.,* 2002 and Hu *et al.,* 2006). Also, PZA has a powerful *in vivo* sterilizing activity, demonstrated both in humans by shortening TB chemotherapy (Mitchison, 1985), as well as in animal models (McCune & Tompsett, 1956; McCune *et al.,* 1956). However, PZA has little or no activity *in vitro* under normal culture conditions at neutral pH (Tarshis *et*

al., 1953). The bactericidal activity of PZA *in vitro* is normally achieved at acid pH, normally around pH 5.5 (McDermott & Tompsett, 1954). PZA activity has also been shown to be considerably enhanced under hypoxic or anaerobic conditions as compared to atmospheric conditions with ambient oxygen (Wade & Zhang, 2004). Nutrient starvation in *M. tuberculosis* has also been shown to cause increased expression of *pncA* and subsequent increase in PZA activity (Betts *et al.,* 2002 and Huan *et al.,* 2007). Additionally, low incubation temperatures (25°C or 22°C) resulted in a considerable increase in the bactericidal activity of PZA (Coleman *et al.,* 2011).

Despite the use of PZA for over six decades, and despite its importance as an irreplaceable component of the TB therapy, its mode of action remains elusive.

2.13 Previously Proposed Models for Mode of Action of PZA

Multiple studies have proposed models for the mechanism of action of PZA. However, the most prevalent ones will be discussed below.

2.13.1 PZA functions as a protonophore, leading to acidification of mycobacterial cytoplasm and loss in membrane potential

The initial foundation for this model stemmed from the apparent essentiality of an acidic pH for PZA action. Under this model, PZA is passively diffused into the *M. tuberculosis* cell, where it is converted to its active form POA, by the bacterial enzyme pyrazinamidase. The active POA accumulates in the cytoplasm of the bacteria and it is expelled from the bacterium by a weak efflux pump that has not yet been identified. Due to the acidity of the extracellular environment outside the bacilli, a fraction of POA (pKa of 2.9) is protonated

and hence becomes charged (HPOA) and can be reabsorbed into the bacterial cytoplasm (pH = 7.2). The proton subsequently dissociates from POA and the entire process is repeated continuously until the pH of the cytoplasm becomes equal to that of the acidic intracellular host environment. The inefficient efflux pump and accumulation of POA inside the bacteria results in disruption of mycobacterial membrane permeability, potential and transport which subsequently leads to cellular damage (Zhang *et al.,* 1999). This model has been supported by several studies (Darby *et al.,* 2013).

This model of POA acting as a protonophore leading to cytoplasmic acidification was recently assessed by our laboratory. Results from this study revealed that, overexpression of *pncA* is able to confer PZA susceptibility to *M. tuberculosis* at neutral and even alkaline culture conditions, but failed to decrease intracellular bacterial pH. Exploiting an *M. tuberculosis* strain which expresses a pH-sensitive green fluorescent protein (GFP), intracellular bacterial pH homeostasis was assessed. From the study, there were no significant changes in the intracellular bacterial pH after treatment with PZA or POA in contrast to treatment with established ionophores, monensin and carbonyl cyanide 3-chlorophenylhydrazone (CCCP) (Peterson *et al.,* 2015).

Finally, using a membrane-permeable fluorescent dye ($DiOC_2$), the membrane potential of *M. tuberculosis* in cells treated separately with POA or CCCP was measured. As expected CCCP resulted in a dramatic loss of membrane potential. However, POA did not significantly alter the membrane potential of *M. tuberculosis* at acidic pH, even at concentration which was ten-fold above the minimum inhibitory concentration (MIC).

From the study, it was concluded that, the ability to uncouple acidic pH from PZA/POA function, lack of cytoplasmic acidification and unremarkable differences in membrane potential in treated and control cells renders this model inviable (Peterson *et al.,* 2015).

2.13.2 PZA disrupts fatty acid synthesis

PZA has also been shown to inhibit the synthesis of fatty acid by targeting mycobacterial fatty acid synthetase I (FAS-I), an enzyme involved in the biosynthesis of lipid (Ciccarelli *et al.,* 2013). Fatty acid synthesis was observed to be disrupted by a structural analogue of PZA, 5- chloropyrazinamide (5-Cl PZA) through the inhibition of fatty acid synthase (FAS- I). Based upon the potent inhibition by 5-Cl PZA it was proposed that PZA was also an inhibitor of FAS-I (Zimhony *et al.,* 2000).

This model has however been questioned in a study by Boshoff *et al.,* where they observed that whole cell assays with either PZA or POA did not inhibit the biosynthesis of fatty acid in *M. tuberculosis*. Also, although 5-Cl-PZA was confirmed as a potent and irreversible FAS-I inhibitor, POA failed to inhibit purified mycobacterial FAS-I (Boshoff *et al.,* 2004). Additionally, POA has an IC_{50} for FAS-I that is over 1000 times greater than that of 5-Cl PZA (Cynamon *et al.,* 1998). Interestingly, unlike PZA, 5-Cl-PZA did not decrease the load of bacteria in the lungs of *M. tuberculosis* infected mice (Ahmad *et al.,* 2012). This suggests that, the two drugs have dissimilar modes of action. As such, PZA is unlikely to target FAS-I directly.

2.13.3 PZA targets pantothenate and coenzyme A synthesis

Our laboratory in a recent study evaluated the activity of PZA against several laboratory strains of *M. tuberculosis* (Dillon *et al.,* 2014). This study revealed that, when mycobacterial cultures are supplemented with pantothenate, pantetheine or β-alanine, the action of PZA as well as its structural analogs is antagonized. These discoveries were consistent with previous studies that showed that, pantothenate synthesis is linked to PZA action (Zhang *et al.,* 2013 and Shi *et al.,* 2014). Nonetheless, when a pantothenate auxotrophic strain was cultured with a sub antagonistic concentration of pantetheine instead of pantothenate, there was an observed restoration of PZA and POA susceptibility. (Dillon *et al.,* 2014). This study further showed that, the action of PZA and POA was not antagonized by β-alanine against the pantothenate auxotrophic strain, showing that this antagonism was specific to pantothenate. This antagonism was confirmed by Gopal *et al.,* who showed that exogenous addition of pantothenate conferred resistance to POA but not to its structural analogs benzoic and nicotinic acid (Gopal *et al.,* 2016).

A recent study has also shown that PZA acts by interacting with CoA metabolism. In this study, Gopal and colleagues revealed that POA reduces CoA in wild-type *M. bovis* BCG (Gopal *et al.,* 2016). Consistent with this observation, our laboratory also showed that treatment of BCG with POA for 24 and 48 hours led to a significant reduction in CoA levels (Rosen *et al.,* 2017). These results insinuate that, targeting the synthesis of pantothenate/CoA is likely to enhance the efficacy of PZA which will possibly result in restoring PZA susceptibility in the resistant isolates with *panD*-linked resistance.

2.14 Resistance to Pyrazinamide

Resistance to PZA is widespread across the world and has been reported in all the six WHO defined regions. Globally, the resistance of *M. tuberculosis* to pyrazinamide has been estimated to be 16% in all TB cases, 60% in individuals with MDR-TB, and 41% in tuberculosis patient who are at high risk of MDR-TB (Whitfield *et al.,* 2015).

2.14.1 Role of *pncA* mutations in PZA resistance

Clinical resistance to PZA occurs in nearly two thirds of the cases through loss of function mutations in *pncA* or its putative regulatory region. Loss of *pncA* function prevents the conversion of PZA to POA thereby inhibiting the enzymatic activation of PZA to active POA that is required for its activity. *M. tuberculosis* is able tolerate the loss of PncA, and its vital role in the NAD salvage pathway, due to its capacity to synthesize NAD *de novo* (Begley *et al.,* 2001; Boshoff *et al.,* 2008). Most of the reported mutations in *pncA* are observed in the 561 bp region of the open reading frame or in an 82 bp region of its flanking region (Scorpio *et al.,* 1996). However, studies have shown that the mutations in *pncA* are very diverse within the MTBC (mycobacterium tuberculosis complex) in different geographical areas (Jure´en *et al.,* 2008; Tan *et al.,* 2014 and Ko¨ser *et al.,* 2014).

Pyrazinamide activity is extremely specific for *M. tuberculosis*, and show minimal or no observed activity against other mycobacteria. For instance, in *M. bovis,* there is a natural substitution of H57A which results in an ineffective PZase, resulting in an inherent resistance to PZA. *M. canettii*, although lacks non-synonymous mutations in *pncA* is also intrinsically resistant to PZA (Scorpio *et al.,* 1997). Correlation of drug resistance phenotypes with mutations in a drug resistance gene has been observed for the other

antitubercular drugs. For instance, the drug resistance phenotype observed for RIF, INH, and EMB, correlates with mutations in the drug resistance genes, *rpoB, katG & inhA* and *embBC* respectively (Zhang & Yew, 2009; Kalokhe *et al.*, 2013). However, PZA appears to have multiple cellular targets resulting in a variable link between PZA resistance and mutations in the *pncA* gene. Other PZA-resistant clinical isolates with intact PZase activity and *pncA* have also been reported in numerous studies, denoting the presence of alternative resistance mechanism(s) or target(s) of PZA (Zhang & Mitchison, 2003).

2.14.2 Role of *panD* mutations in PZA resistance

Mutations in *panD*, encoding aspartate-decarboxylase, an enzyme involved in the synthesis of β-alanine, a precursor for pantothenate and coenzyme A biosynthesis (Figure 2.6), has been proposed to be a target of PZA. Zhang and colleagues isolated 174 *in vitro* generated isogenic mutants of *M. tuberculosis* H37Rv that showed resistance to PZA and characterized them by whole genome sequencing, to identify novel mutations in their genomes. The sequence analyses identified 5 low level PZA-resistant mutants which had mutations in *panD (*Zhang *et al.*, 2013). A follow-up study by the same group showed the presence of *panD* mutations in 27 POA-resistant mutants. All the *panD* mutations identified, affected the C-terminus of the *panD* protein, with PanD M117I mutant being the highest occurring mutation. They also observed overexpression of *panD* in resulted in PZA and POA resistance in an *M. tuberculosis* strain. Furthermore, they discovered that the POA inhibited the activity of *M. tuberculosis panD* enzyme in a concentration-dependent manner. This enzyme inhibition was however not realized with PZA or with a control compound nicotinamide, suggesting that *panD* is a target of PZA/POA (Shi *et al.*,

2015). Another study also identified missense mutations in *panD* in POA resistant mutants of *M. bovis* BCG (Gopal *et al.,* 2016).

Conversely, our laboratory found that a *panC and panD* double knockout mutant of *M. tuberculosis* maintained susceptibility to PZA when cultured with a sub-antagonistic concentration of pantetheine. This shows that *panD* is not likely to be the primary target for PZA. This result therefore uncouples PZA action with pantothenate synthesis, demonstrating that pantothenate-mediated antagonism arises through a different mechanism that does not require *panD* (Dillon *et al.,* 2014).

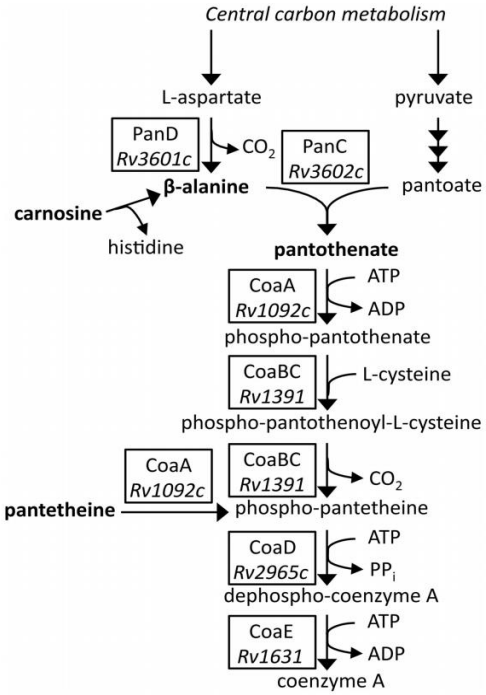

Figure 2.6: Coenzyme A biosynthetic pathway of *Mycobacterium tuberculosis*. The triple arrow represents the sequence of reactions from pyruvate to pantoate. Proteins that catalyze the respective reactions are represented in boxes. The italicized Rv numbers represent H37*Rv* genes that encode the proteins. The boldface metabolites are those found to antagonize PZA (Dillon *et al.,* 2014).

2.14.3 Role of *rpsA* in PZA resistance:

In a search for molecular targets of POA, Shi and colleagues reported a novel target of POA as *rpsA*, which encodes the 30S ribosomal protein S1, a fundamental protein involved in *trans*-translation, a mechanism used by bacteria to release stalled ribosomes that on mRNA transcripts (Shi *et al.,* 2011). This study was enacted based upon the low level PZA resistance seen in the *M. tuberculosis* clinical isolate DHMH444 that lacked *pncA* mutations (Scorpio *et al.,* 1997). Later, sequence analysis of the *rpsA* from the DHM444 strain revealed that it contained a ΔA438 deletion at the C-terminus of RpsA. Furthermore, they overexpressed and purified the mutant RpsA ΔA438 protein. Using isothermal titration calorimetry, they observed direct binding between POA and RpsA, and inhibition of *trans*-translation in a cell free assay. Other studies have also supported this model (Tan *et al.,* 2014; Ilina *et al.,* 2013).

Nevertheless, this model has recently been refuted by our laboratory. Utilizing isogenic laboratory strain of *M. tuberculosis (*H37Ra), the impact of RpsAΔA438 was assessed. Reconstruction of the RpsAΔA438 polymorphism in PZA susceptible H37Ra strain revealed that, there was no distinguishable difference between the minimum inhibitory concentration (MIC) of this strain in comparison to parental strain. It was therefore concluded that the RpsAΔA438 polymorphism is not linked with PZA susceptibility (Dillon *et al.,* 2017). The PZA resistant DHMH444 strain has also been found to maintain full susceptibility to POA in broth culture (Speirs *et al.,* 1995) and in a murine model of TB infection (Klemens *et al.,* 1996). Furthermore, over-expression of *rpsA* did not confer PZA resistance in *M. tuberculosis* H37*Ra*. In addition, re-analysis of transcriptional array data from Boshoff *et al.,* (2004), showed that expression levels of *rpsA* were relatively

unchanged between PZA treated *M. tuberculosis* and no drug control, even at 1x and 10x the MIC of PZA. Also, using isothermal titration calorimetry, no interaction was observed between *M. tuberculosis* RpsA and POA. Finally, utilization of an *in vitro trans*-translation assay shows that, POA does not inhibit *trans*-translation in *M. tuberculosis* (Dillon *et al.*, 2017).

2.15 Pyrazinamide Susceptibility Testing

Employing PZA susceptibility testing *in vitro* by conventional agar-based methods often leads to unclear results. This is due to poor buffering capacity of the test media, the use of an acidic medium pH that prevents the growth of bacilli, and the use of extremely large inocula that increase the pH of the media, resulting in the reduced activity of PZA, thus leading to false resistance (Tummon., 1975). In addition, results of conventional methods of PZA susceptibility can take more than 2 weeks to be obtained (Vandal *et al.*, 2008).

BACTECT MGIT (mycobacterial growth indicator tube) 960 system (Becton Dickinson, Sparks, MD), test for pyrazinamidase activity has been used as the gold standard to measure PZA drug susceptibility *in vitro*. This system however, has generated varying test outcomes (Louw *et al.*, 2006). The Wayne test, a colorimetric test of pyrazinamidase activity is used as an alternative, though results are sometimes difficult to interpret (Wayne, 1974). Additionally, molecular detection of PZA resistance-related mutations in *pncA* has also been used as a molecular marker for PZA resistance (Scorpio and Zhang, 1996). However, about one third of PZA resistant clinical isolates have no *pncA* mutations.

Bearing in mind the above-mentioned challenges with existing methods, it is imperative to

obtain rapid, reliable, and most importantly, affordable test methods for the detection of PZA resistance, especially in resource limited settings where MDR-TB is on the rise.

CHAPTER 3

3.0 METHODOLOGY

3.1 Transposon Mutagenesis to Isolate POA Resistant Mutants

Transposon mutagenesis was carried out using a mycobacteriophage containing *Himar1* mariner transposon and a kanamycin resistant cassette (*kanR*).

3.1.1 Bacterial strains and growth media

M. tuberculosis vaccine strain, M. *bovis*, Bacillus Calmette–Guérin (BCG) and *M. smegmatis* mc^2155 were kind gifts from W.R. Jacobs, Jr. of the Albert Einstein College of Medicine. BCG was grown in Middlebrook 7H9 liquid or 7H10 agar medium (Difco) supplemented with 0.2% (vol/vol) glycerol (Macron fine chemicals), 10% (vol/vol) oleic acid-albumin-dextrose-catalase (OADC) (Difco), and 0.05% (vol/vol) tyloxapol (Sigma Aldrich). *M. smegmatis* mc^2155 was grown in Middlebrook 7H9 medium (Difco) supplemented with 20% (vol/vol) dextrose (EM Science) and 0.05% (vol/vol) tyloxapol.

3.1.2 Preparation of Middlebrook 7H9 liquid medium for growth of BCG and H37Ra

A volume of 1 liter Middlebrook 7H9 (M7H9) liquid medium was prepared by dissolving 4.7 g of M7H9 powder in 900 ml of milliQ ultrapure water. A volume of 100 ml OADC, 4 ml 50% glycerol and 2.5 ml 20% tyloxapol were added to the mixture. The resulting mixture was filtered through a 0.22 µm membrane filter (Millex) and subsequently stored at 4°C.

3.1.3 Preparation of Middlebrook 7H10 agar medium for growth of BCG and H37Ra

A volume of 1 liter Middlebrook 7H10 (M7H10) agar medium was prepared by dissolving 19 g of M7H10 agar powder in 900 ml of milliQ ultrapure water. The mixture was autoclaved at 121°C for 15 minutes, after which the media was cooled to 55°C. A volume of 100 ml OADC and 4 ml 50% glycerol were added to the cooled media, mixed and 20 ml of the media was aliquoted into petri dishes and subsequently stored at 4°C.

3.1.4 Preparation of Middlebrook 7H9 liquid medium for growth of *M. smegmatis* mc^2155

A volume of 1 liter M7H9 liquid medium was prepared by dissolving 4.7 g of M7H9 powder in 1 liter of milliQ ultrapure water. A volume of 10 ml of 20% dextrose and 2.5 ml 20% tyloxapol were added to the mixture and the resulting mixture was filtered through a 0.22 µm membrane filter and subsequently stored at 4°C.

3.1.5 Preparation of Middlebrook 7H10 agar medium for growth of *M. smegmatis* mc^2155

A volume of 1 liter M7H10 agar medium was prepared by dissolving 19 g of M7H10 agar powder in 1 liter of milliQ ultrapure water. The mixture was autoclaved, after which the media was cooled to 55°C. A volume of 10 ml 20% dextrose was added to the cooled media, mixed and then 20 ml of the media was aliquoted into petri dishes and subsequently stored at 4°C.

3.1.6 Preparation of noble agar

Noble agar is an agar overlay used during mycobacteriophage propagation. A 500 ml

volume of noble agar was prepared by dissolving 2.34 g of M7H9 powder and 3.75 g of noble agar powder (Difco) in 500 ml of milliQ ultrapure water. The mixture was autoclaved and subsequently stored at RT. The noble agar was melted in a microwave prior to its use.

3.1.7 Preparation of Luria Bertani (LB) broth for growth of *Escherichia coli*

A volume of 1 liter LB broth was prepared by dissolving 25 g of LB powder (Invitrogen) in 1 liter of milliQ ultrapure water, autoclaved and then stored at RT.

3.1.8 Preparation of Luria Bertani agar for growth of *Escherichia coli*

A volume of 1 liter LB broth was prepared by dissolving 25 g of LB powder and 15 g of agar powder (Invitrogen) in 1 liter of milliQ ultrapure water. The mixture was then autoclaved, after which the media was cooled to 55°C. A volume of 20ml of the media was aliquoted into petri dishes and subsequently stored at 4°C.

3.1.9 Preparation of chemically competent *M. smegmatis* mc^2155

Chemically competent *M. smegmatis* mc^2155 was prepared by harvesting culture of optical density $(OD)_{600}$ between 0.6-0.8 at 3000 rpm for 10 minutes at room temperature (RT). The pellet was re-suspended and washed twice in equal volume of mycobacteriophage (MP) buffer (50 mM Tris, 10 mM $MgCl_2$, 150 mM NaCl, and 2 mM $CaCl_2$) (Mallinckrodt). The washing procedure was repeated with ½ volume of MP buffer, after which the pellet was finally suspended in $1/10^{th}$ volume of MP buffer. A volume of 400 µl of the chemically competent cells was added to 100 µl of 50% glycerol and stored at -80°C.

3.1.10 Preparation of high titer *Himar1* mariner transposon phage

One hundred microliters (100 µl) of competent *M. smegmatis* mc^2155 was mixed with 3 ml noble agar and plated on supplemented M7H10 agar. A range of ten-fold serial dilutions of the phage were made and 5 µl of 10^0 through 10^{-10} dilutions were spotted onto the above plate and incubated at 30°C for 2 days.

Phage titer in plaque forming units per milliliter (pfu/ml) was calculated as

$$Phage\ titer\ \left(\frac{pfu}{ml}\right) = \frac{number\ of\ plaques\ observed}{dilution\ factor\ \times volume\ of\ phage\ spotted}$$

The dilution with approximately 1000 plaques was further propagated by adding a 100 µl each of the phage and competent *M. smegmatis* mc^2155 to 3 ml noble agar in a snap cap tube. This was mixed by vortexing and subsequently plated on supplemented M7H10 agar medium and incubated at 30°C for 2 days to obtain plaques. The phage was harvested by flooding the plates with 5 ml MP buffer and placed on a shaker for 5 hours at RT. The phage lysate was harvested and filtered through 0.22 µm membrane filter and the titer was determined as described above. This assay was repeated until a phage titer of approximately 10^{10} pfu/ml was obtained.

3.1.11 Transposon mutagenesis

A 10 ml mid-log BCG culture of OD_{600} 0.6-0.8 was harvested at 3000 rpm for 10 minutes at RT. The pellet was re-suspended and washed in 10 ml MP buffer at 3000 rpm for 10 minutes at RT. Subsequently, the pellet was suspended in 1 ml of high titer phage preheated to 37°C and then incubated at 37°C for 24 hours. BCG culture suspended in MP buffer with no phage served as a control. The transposon mutagenized and control bacilli were further re-suspended in 1 ml of supplemented M7H9 medium. A volume of 100 µl was

subsequently plated on M7H10 agar medium containing 50 µg/ml kanamycin and pyrazinoic acid (POA) (Sigma Aldrich) of different concentrations at pH 6.8. A control plate which contained kanamycin but NO POA was also set up. The plates were incubated at 37°C for 14 days. A total of 77 and 3 transposon mutants were selected from the POA and kanamycin plates respectively, and were cultured in 30ml square bottles (Nalgene) containing supplemented M7H9 medium with kanamycin (Table 3.1).

Table 3.1: Number of transposon mutants selected from respective POA plates

POA conc. (µg/ml)	0	37.5	75	150	300	600	1200	2400
Number of mutants selected	3	7	10	10	20	20	4	6

3.1.12 Antimycobacterial susceptibility determinations

To test if the selected transposon mutants were resistant to 200 µg/ml POA (MIC_{90} for wild type BCG at pH 6.8), each mutant was grown to mid-exponential phase (OD_{600} 0.6 – 0.8) in supplemented M7H9 medium. The cells were diluted to an OD_{600} of 0.01 in supplemented M7H9 (pH 6.8) with 200 µg/ml POA and 50 µg/ml kanamycin in a 96 well plate. A control plate with no POA was also set aside. The plates were incubated at 37°C for 21 days, after which the OD_{600} of each well was measured and recorded. Mutants that had $\frac{\mathrm{OD}_{600}\,(POA)}{\mathrm{OD}_{600}\,(NO\ POA)} > 0.5$ were termed resistant.

Again, the mutants' susceptibility to POA was determined on an agar medium by spotting 2 µl of the exponential phase (OD_{600} of 0.6 – 0.8) bacteria on supplemented M7H10 agar (pH 5.8) containing 50 µg/ml, 100 µg/ml, 200 µg/ml, 400 µg/ml and 800 µg/ml of POA. A NO POA control plate was also set up for the assay. The plates were incubated at 37°C for 21 days. Minimum inhibitory concentration (MIC_{90}) was defined as the minimum concentration of POA required to inhibit 90% of the visible bacterial growth on POA plates as compared to the no drug control.

Also, four randomly selected resistant mutants were taken through POA susceptibility testing in liquid medium at pH 6.8 to determine their $MIC_{90.}$ Briefly, exponentially growing (OD_{600} 0.6-0.8) transposon mutants and wild type strains were diluted to an OD_{600} of 0.01 in 5 ml of supplemented M7H9 medium. POA was added to final concentrations of 50 µg/ml, 100 µg/ml and 200 µg/ml. A no POA control was also set up. Cultures were incubated in a shaking incubator at 37°C for 14 days. Following incubation, the MIC_{90} of each culture was determined. MIC_{90}, was defined as the minimum concentration of POA that inhibits 90% of growth relative to the no drug control. All experiments were carried out in triplicate.

3.1.13 Genomic DNA extraction

Genomic DNA was extracted from the four randomly picked POA resistant transposon mutants. A 5ml volume of each culture with an OD_{600} of approximately 2.0 were pelleted, then resuspended and washed in 250 µl GTE (10 mM EDTA, 25 mM Tris pH 7.9 and 50 mM glucose). The cells were then lysed in 225 µl of GTE and 25 µl of 10 mg/ml lysozyme

and further incubated at 37°C for 3 hours. Following incubation, 50 µl of 10% SDS together with 25 µl of 10 mg/ml proteinase K were added and the mixture was incubated at 55°C for 30 minutes. Subsequently, 100 µl of 5 M NaCl and 80 µl of CTAB saline solution (0.7 M NaCl, 0.275 M hexadecyl- trimethylammonium bromide) were added and the samples were incubated for 10 minutes at 65°C. DNA was extracted using 500 µl chloroform:isoamyl alcohol (24:1) treatments twice. During each extraction, the lower organic phase was discarded. The DNA was then precipitated from the aqueous phase with 300 µl isopropanol (Sigma Aldrich) and washed with 500 µl 70% ethanol prior to its resuspension in 50 µl EB buffer (Qiagen). The concentration of the DNA was measured using a Nanodrop spectrophotometer (Thermo scientific Nanodrop 2000).

3.1.14 Transformation of *E. coli*

A 100 µl volume of competent DH5 α *E. coli* was thawed on ice, after which 5 µl of plasmid DNA (100 ng) was added to the cells and mixed. The mixture was then placed on ice for 30 minutes. Subsequently, the mixture was heat shocked at 42°C for 45 seconds and then placed on ice to recover for 2 minutes. A 1ml volume of room temperature LB broth was added to the mixture which was placed in a shaking (250 rpm) 37°C incubator for 1 hour. Following incubation of transformed *E. coli*, LB agar selection plates supplemented with kanamycin were pre-warmed to 37°C, after which 100 µl of the transformed cells were plated and incubated overnight at 37°C.

3.1.15 Identification of transposon insertion site

A 10 µl volume of the extracted genomic DNA (gDNA) from the POA resistant mutants was digested with the restriction enzyme *BssHII* (New England Biolabs, NEB) at 50°C for

3 hours in a 20 µl reaction (10 µl gDNA, 2 µl 10x NEB CutSmart Buffer, 1 µl *BssHII* and 7 µl nuclease free water). The restriction enzyme was heat inactivated at 65°C for 20 minutes and entire digested product was then ligated in a 25 µl reaction (20 µl digestion reaction, 2.5 µl 10x NEB T4 DNA ligase buffer, 0.5 µl T4 DNA ligase and 2 µl nuclease free water) overnight at RT. A 5 µl volume of the ligated product was used to transform 100 µl of *E. coli* DH5 λ pir and then the transformed cells were plated on LB agar plates supplemented with kanamycin and incubated overnight at 37°C. Six colonies were selected, and cultured overnight at 37°C in LB broth containing 50 µg/ml kanamycin. Plasmid DNA was prepared using Qiagen QIAprep spin Miniprep kit, following manufacturer's protocol, and purified plasmids were subjected to Sanger sequencing using the Kan_Rev_Seq primer (Table A1 in appendix), which was oriented outward from the 3' end of the *mariner* kanamycin resistance cassette such that the adjacent chromosomal DNA was sequenced. The resulting sequences were aligned with *M. bovis* BCG genome (GenBank accession number NC_002945.3) to identify the insertion sites. Further, the remaining POA resistant transposon mutants were pooled, and gDNA was extracted and submitted for next generation sequencing.

3.2 Checkerboard Assay to Test for Synergy between Pyrazinamide (PZA) and Hydrogen Peroxide (H_2O_2)

3.2.1 Bacterial strains and growth media

Attenuated *M. tuberculosis* strain H37*Ra*, *M. bovis* strains BCG and BCG-*pncA* (wild type BCG with *pncA* ectopically expressed) were gifts from W.R. Jacobs of the Albert Einstein College of Medicine. The strains were cultured in M7H9 liquid medium (Difco) containing

10% albumin-dextrose-sodium chloride (ADS), 0.2% (vol/vol) glycerol and 0.05% (vol/vol) tyloxapol.

3.2.2 Preparation of ADS

A 500 ml volume of ADS was prepared by dissolving 25.0 g of bovine serum albumin (BSA) (Invitogen), 10 g dextrose powder and 4.25 g of NaCl in 500 ml of milliQ ultrapure water. The resulting mixture was filtered through a 0.22 µm membrane filter and subsequently stored at 4°C.

3.2.3 Determination of Minimum inhibitory concentration (MIC) and fractional inhibitory concentration (FIC)

Drug susceptibility was determined for H37*Ra*, BCG and BCG-*pncA* by measuring OD_{600} of the strains grown with varying concentrations of drug. Synergy between the varying combinations of PZA (MP Biomedicals) and H_2O_2 (Macron Fine chemicals) was determined by setting up checkerboard assays. Checkerboard assays allow for testing many combinations of drugs at different ratios. Setting up this type of assay allows us to calculate the individual impact of each drug alone (MIC_{90}) and in combination (fractional inhibitory concentration, FIC). Briefly, exponentially growing mycobacterial strains were diluted to an OD_{600} of 0.01 in 5 ml of supplemented M7H9 medium (pH 5.8) containing varying PZA concentrations (0, 3.125 µg/ml, 6.25 µg/ml, 12.5 µg/ml, 25 µg/ml, 50 µg/ml and 100 µg/ml) in 30 ml square bottles. The cultures were incubated at 37°C on a 100 rpm rotary shaker for 72 hours. Following incubation, the mycobacterial cells were diluted to an OD_{600} of 0.01, after which they were challenged with different concentrations of H_2O_2 (0, 0.039 mM, 0.078 mM, 0.156 mM, 0.3125 mM, 0.625 mM and 1.25 mM) and further incubated

at 37°C on a 100 rpm rotary shaker for 14 days. The FIC for each compound was defined as the lowest amount of compound required to inhibit 90% of the bacterial growth as compared to untreated cultures upon concurrent exposure to a constant concentration of the other compound. This is shown below.

$FIC[PZA] = [PZA]/MIC_{PZA\ alone}$ $FIC[H_2O_2] = [H_2O_2]/MIC_{H2O2\ alone}$

The fractional inhibitory concentration index (FICI) was determined by calculating the sum of the measured FIC values for each compound at each point and then reporting the lowest value determined.

$FICI = FIC[PZA] + FIC[H_2O_2]$

$FICI \leq 0.5$ is termed synergy, $FICI = 1$ is termed additive and $FICI > 4$ is termed antagonism

All MIC and FIC assays were conducted in triplicate.

Table 3.2: Setup for checkerboard assay to test synergy between PZA and H_2O_2

	H_2O_2 (mM)						
PZA µg/ml	**0**	**0.039**	**0.078**	**0.156**	**0.3125**	**0.625**	**1.25**
100	**COMBINATION OF PZA and H_2O_2**						
50							
25							
12.5							
6.25							
3.125							
0							

3.3 Construction of *aceE* Knockout Mutant

I attempted to construct an *aceE* knockout mutant using a modified version of specialized transduction method of allelic exchange and gene deletion in mycobacteria (Bardarov *et al.*, 2002 and Jain *et al.*, 2014).

3.3.1 Preparation of electrocompetent mycobacteria cells

Electrocompetent *M. smegmatis* mc^2155, BCG and H37*Ra* were prepared by centrifuging culture of OD_{600} between 0.6-0.8 at 3000 rpm for 10 minutes at RT. The pellet was re-suspended and washed twice in equal volume of 10% glycerol and again with half volume of 10% glycerol. The pellet was finally suspended in $1/10^{th}$ volume of 10% glycerol and split into 400 µl aliquots which were stored at -80°C.

3.3.2 Construction of allelic exchange substrate (AES)

The *in silico* allelic exchange substrate (AES) was constructed via Gibson Assembly using neBuilder Assembly Tool by New England Biolabs. Briefly, 850 bp upstream and 851 bp downstream chromosomal sequences flanking the *aceE* coding DNA sequence (CDS) were designed to flank the hygromycin resistance (*hygR*) and *sacB* cassette of the plasmid p0004S. The *hygR* and *sacB* cassettes are represented as the insert, and the remaining plasmid sequence is designated as backbone. The assembly tool then generated primers (Table A1, appendix) as well as the final *in silico* AES. The primers were then used to amplify the pieces for the assembly using PCR (Bio Rad T100 Thermal cycler) in which H37Ra genomic DNA and p0004S purified plasmid served as template. The PCR products were confirmed on a 1% agarose gel.

Afterwards, Qiagen QIAquick PCR purification cleanup kit was used to purify the amplicons following the manufacture's protocol. The products amplified from p0004S were digested via the *DpnI* restriction digest at 37°C for 1 hour to digest methylated DNA. The enzyme was then inactivated at 80°C for 20 minutes. An assembly reaction involving four-piece ligation (p0004S *hygR* and *sacB* cassettes, p0004S backbone, H37*Ra aceE* upstream sequence, and H37*Ra aceE* downstream sequence) was set up following the master mix protocol. Then, 10 µl of the assembly reaction was used to transform 100 µl competent DH5 α *E. coli*, cultured on LB plates supplemented with 150 µg/ml hygromycin and incubated overnight at 37°C. The restriction enzymes *XhoI* and *HpaI* (NEB) (selected from the restriction enzyme map of p0004S using Clone manager software) were then used to digest plasmid extracted from hygromycin resistant colonies, and the resulting digestion reactions were screened on a 1% agarose gel to verify the banding pattern and thus, proper construction of the AES. Candidate plasmids were screened on a 1% agarose gel after digestion with *XhoI* and *HpaI* at 37°C for 1 hour. The gel confirmed plasmids strains were sequenced verified and compared with the *in silico* AES generated using Geneious sequence analysis software.

Table 3.3: A representative PCR reaction mix

Component	50 µl reaction	Final concentration
5X Phusion GC Buffer	10 µl	1X
10 mM dNTPs	1 µl	10 µM
10 µM Forward Primer	2.5 µl	10 µM
10 µM Reverse Primer	2.5 µl	10 µM
Template DNA	1 µl	< 250 ng
DMSO	1.5 µl	3%
Phusion DNA polymerase	0.5 µl	1.0 units / 50 µl reaction
Nuclease free water	31 µl	

Table 3.4: Polymerase Chain Reaction (PCR) Conditions

STEP	Temperature (°C)	Duration
1. Initial denaturation	98	30 seconds
2. Denaturation	98	10 seconds
3. Annealing	Primer annealing temperature	15 seconds
4. Extension	72	15-30 seconds per kb
5. Final extension	72	5 minutes
6. Cooling	4	-

Steps 2-4 were repeated for 35 cycles. After the amplification, 2 µl of 6X loading dye (NEB) was added to 10 µl of each PCR product and run on a 1 % agarose gel (containing 3 µl of 10 mg/ml ethidium bromide (Invitrogen)) at 200 V for 30 minutes.

3.3.3 Preparation of HB101 *E. coli* for transduction

E. coli HB101 was grown overnight at 37°C in LB broth supplemented with 0.2% maltose and 10 mM MgSO4. Afterwards, 25 ml of fresh medium was inoculated with 0.5 ml of the overnight culture and the mixture was then incubated in a shaking incubator (200 rpm) at 37°C until OD_{600} of 0.8-1.0 was reached. The cells were then harvested by centrifugation at 3000 rpm, 4°C for 10 minutes. The pellets were resuspended in 12.5 ml 10 mM MgSO4 and stored at 4°C.

3.3.4 Phasmid Construction

Confirmed AES and phasmid phAE159 DNA were both digested with *PacI* (NEB) at 37°C for 2 hours and the enzyme was inactivated at 65°C for 20 minutes. The digested phasmid phAE159 was phosphatase treated using Antarctic phosphatase (NEB) following manufacturer's protocol. The digested products were subsequently ligated and the ligation product was packaged *in vitro* using a MaxPlax bacteriophage lambda packaging extract. Briefly, 25 µl of the extract was added to 10 µl of the ligation mix and incubated at RT for 2 hours, after which the reaction was stopped with 400 µl of MP buffer. The mixture was incubated again at RT for 30 minutes. Following the incubation, 1 ml of *E. coli* HB101 was added to the packaging mixture and subsequently incubated at 37°C for 1 hour in a shaking incubator. After the stipulated time of incubation, the cells were centrifuged at 13,000 rpm for 1 minute. The pellets were resuspended in 1 ml LB broth and 100 µl of the resulting cells were plated onto LB selection plates containing 150 µg/ml hygromycin (Invitrogen) and incubated overnight at 37°C. The resulting phage was used to transduce *E. coli* HB101. The colonies obtained were screened for potential phasmid by DNA extraction and digestion with *PacI* restriction enzyme at 37°C for 2 hours. The digested

products were run on a 1% agarose gel to confirm the band pattern.

3.3.5 Mycobacteriophage preparation

A volume of 10 µl confirmed phasmid was electroporated into 400 µl electrocompetent *M. smegmatis* mc^2155 cells for mycobacteriophage propagation. The transformed cells were then added to 3 ml noble agar and subsequently plated on supplemented M7H10 agar containing hygromycin. The plates were incubated at 30°C for 3 days after which the phage plaques were cored out into 200 µl MP buffer to recover the phage. The resulting phage was then propagated in *M. smegmatis* mc^2155 as previously described until a phage titer of 10^{10} pfu/ml was attained.

3.3.6 Transduction

High titer phage was used to transduce *M. bovis* BCG and *M. tuberculosis* H37*Ra*. Briefly, 10 ml mid-log cultures of OD_{600} 0.6-0.8 were harvested at 3000 rpm for 10 minutes at RT. The pellet was re-suspended and washed in 10 ml MP buffer at the same conditions. Subsequently, the pellet was suspended in 1 ml of high titer phage preheated to 37°C and then incubated at 37°C for 24 hours. Cultures suspended in MP buffer with no phage served as a control. The transduced and control bacilli were further re-suspended in a milliliter of supplemented M7H9 medium. A volume of 100 µl was subsequently plated on M7H10 hygromycin selection plates containing 0.05% glutamic acid and incubated at 37°C for 4 weeks. Colonies were selected and further cultured in supplemented M7H9 medium containing 150 µg/ml hygromycin and 0.05% glutamic acid (Sigma Aldrich).

3.4 Overexpression of *pckA* to Determine Increased Susceptibilty to Pyrazinoic Acid (POA)

3.4.1 Construction of *pckA* overexpression strain

pckA was amplified from BCG genomic DNA by PCR with primers containing *HindIII* and *NheI* restriction sites at the 5' and 3' ends of the gene respectively. The PCR amplicons were run on a 1% agarose gel to verify fragment size prior to purification using Qiagen QIAquick PCR purification kit. A concentration of 500 ng of each purified PCR product and the constitutive replicating pUMN002 plasmid were digested at 37°C for 1 hour in a 25 µl reaction containing *HindIII* and *NheI* restriction enzymes. The digestion pattern was confirmed on a 1% agarose gel and the pUMN002 plasmid fragment was phosphatase treated using Antarctic phosphatase (NEB) following manufacturer's protocol. The insert DNA was ligated into the plasmid at an insert to vector ratio of 3:1 overnight at RT and 5 µl of ligation product was transformed into 100 µl competent DH5 α *E. coli*, plated on LB agar plates containing 50 µg/ml kanamycin, and incubated at 37°C overnight. Selected colonies were cultured overnight and plasmid DNA was extracted using the Qiagen QIAprep spin Miniprep kit, following manufacturer's protocol. Plasmid DNA was digested with *HindIII* and *NheI* and the products were run on a 1% agarose gel to confirm correct band pattern. Plasmids with the correct pattern was sequence confirmed using pT_For and pT_Rev primers (Table A1, appendix) and 5 µl of the sequence verified plasmids were electroporated into 400 µl electrocompetent *M. bovis* BCG and H37*Ra* with a pulse 2.5 KV, 100 Ω and 25 µF (Bio Rad Gene Pulser II). A volume of 100 µl of the electroporated cells were plated on supplemented M7H10 agar plates containing 50 µg/ml kanamycin (Invitrogen) and incubated at 37°C for 14 days. Following incubation, colonies were

selected and grown in M7H9 broth containing 50 µg/ml kanamycin in shaking incubator for 7 days. The cultures underwent colony PCR using GoTaq Green Master Mix (Promega) following manufacturer's protocol and Kan_For and Kan_Rev primers (Table A1, appendix) to verify the presence of the kanamycin resistant cassette and thus, the *pckA* overexpression construct. The PCR products were confirmed on a 1% agarose gel.

3.4.2 RNA extraction

For quantification of *pckA* expression, RNA was extracted from both BCG and H37*Ra* overexpression strains as well as wild type strains using trizol extraction. Briefly, a 15 ml volume of mid-exponential phase (OD_{600} 0.5-0.8) cultures were pelleted by centrifugation at 4000 rpm for 10 minutes at 4°C. The pelleted cells were resuspended in 500 µl TriReagent (Invitrogen) with 1% polyacryl carrier (Molecular research center). The RNA in the cells was extracted by bead beating twice (1 minute each, with a 2 minute break on ice) with 250 µl of 0.1 mm zirconia beads (BioSpec). The supernatant was transferred into screw cap tubes and 50 µl of 1-Bromo-3-chloropropane (BCP) (Sigma Aldrich) was added and incubated at RT for 10 minutes. Following incubation, each sample was centrifuged at 10,000 rpm for 15 minutes at 4°C. The upper aqueous phase containing the RNA was collected and 250 µl of isopropanol was added, incubated at RT for 10 minutes and then the RNA was pelleted at 10,000 rpm for 15 minutes at 4°C. The RNA was further washed with 300 µl of 70% ethanol prior to its resuspension in 50 µl of RNase free water (Gene Mate). The extracted RNA was stored at 4°C overnight, to allow the RNA to dissolve. After the overnight incubation, the RNA was re-extracted again as described earlier. The RNA was stored in -80°C until ready to use.

3.4.3 Quantitative Reverse Transcription Polymerase Chain Reaction (qRT-PCR)

For quantification of *pckA* expression, qRT-PCR was performed. Following the RNA extraction, 4 µg of each RNA sample was taken through DNase treatment in a 25 µl reaction at 37 °C for 30 minutes using Turbo DNase Kit (Invitrogen) following manufacturer's protocol, to remove the remaining DNA from the sample. After the DNase treatment, qRT-PCR was performed using QuantiFast SYBR Green RT-PCR kit (Qiagen). Each reaction mix was prepared with 5 µl of 2X QuantiFast SYBR Green RT-PCR master mix (Qiagen), 1 µl of 10 µM of pckA_qrt_For and pckA_qrt_Rev primers (Table A1, appendix), 0.1 µl QuantiFast RT Mix and 1 ng RNA. A volume of 10 µl of the reaction mix for each sample was aliquoted in duplicate into 96 well plate (Roche) and subsequently run on a LightCycler 480. A negative control, without reverse transcriptase was run alongside to check for gDNA contamination of the RNA prep. The expression level of *pckA* was normalized to mycobacterial sigma factor *SigA* using sigA_For and sigA_Rev primers (Table A1, appendix). The real time cycling conditions used included reverse transcription step at 50°C for 10 min, PCR initial activation step at 95°C for 5 min, 35 cycles of denaturation step at 95°C for 10 seconds, combined annealing/extension step at 60°C for 30 seconds, with fluorescence quantification for each cycle. The cycle threshold (Ct) value was used to calculate the fold change in expression of *pckA* in each reaction mix. For a real-time PCR assay, a positive reaction is identified by the presence of a fluorescent signal. The Ct value is therefore defined as the cycle at which fluorescence from amplification exceeds the background fluorescence.

The fold change in *pckA* expression relative to *SigA* expression was calculated using the equation

Fold change = 2^-dd; where dd = dTE-dTC

dTE = (Average Ct value of *pckA* in each mutant strain) - (Average Ct value of *sigA* in each mutant strain)

dTC = (Average Ct value of *pckA* in each wild type strain) - (Average Ct value of *sigA* in each wild type strain)

3.4.4 POA susceptibility testing

Exponentially growing (OD_{600} 0.6-0.8) *pckA* overexpression mutant strains as well as wild type strains were diluted to an OD_{600} of 0.01 in 5 ml of supplemented M7H9 medium adjusted to pH 5.8 and pH 6.8. For pH 6.8 cultures, POA was added to final concentrations of 50 µg/ml, 100 µg/ml and 200 µg/ml. Final POA concentrations for pH 5.8 cultures were 12.5 µg/ml, 25 µg/ml and 50 µg/ml. For both culture conditions, a no POA control was made. Cultures were incubated in a shaking incubator at 37°C for 14 days. Following incubation, POA susceptibility was determined by determining the MIC_{90} of the respective cultures. All experiments were carried out in triplicates.

CHAPTER 4

4.0 RESULTS

4.1 Transposon mutagenesis and recovery of POA resistant mutants

It was recently found in our laboratory that bacteriophage infection potentiates PZA susceptibility in *M. tuberculosis* H37*Rv* (unpublished results). In order to gain a better understanding of PZA susceptibility, we sought to identify PZA resistance conferring mutations in *M. tuberculosis.* The model organism used was attenuated *M. bovis* vaccine strain Bacillus Calmette–Guérin (BCG). This was achieved by using a *Himar1* mariner based transposon mutagenesis. Like all *M. bovis* strains, BCG is naturally resistant to PZA due to a loss of function mutation in *pncA*, which encodes the nicotinamidase responsible for converting PZA to POA. As such, the transposon library was used to select for POA resistance. The transposon mutants were plated on agar plates without POA as well as sub-inhibitory concentrations of POA to ascertain if phage infection potentiates POA action in BCG. From the data, it was observed that phage infection sensitized BCG to POA up to about 32 fold. This was seen in the reduction of the agar MIC_{90} (pH 6.8) of the transposon mutants to 75 µg/ml as opposed to the wildtype MIC_{90} of over 2000 µg/ml (Figure 4.1).

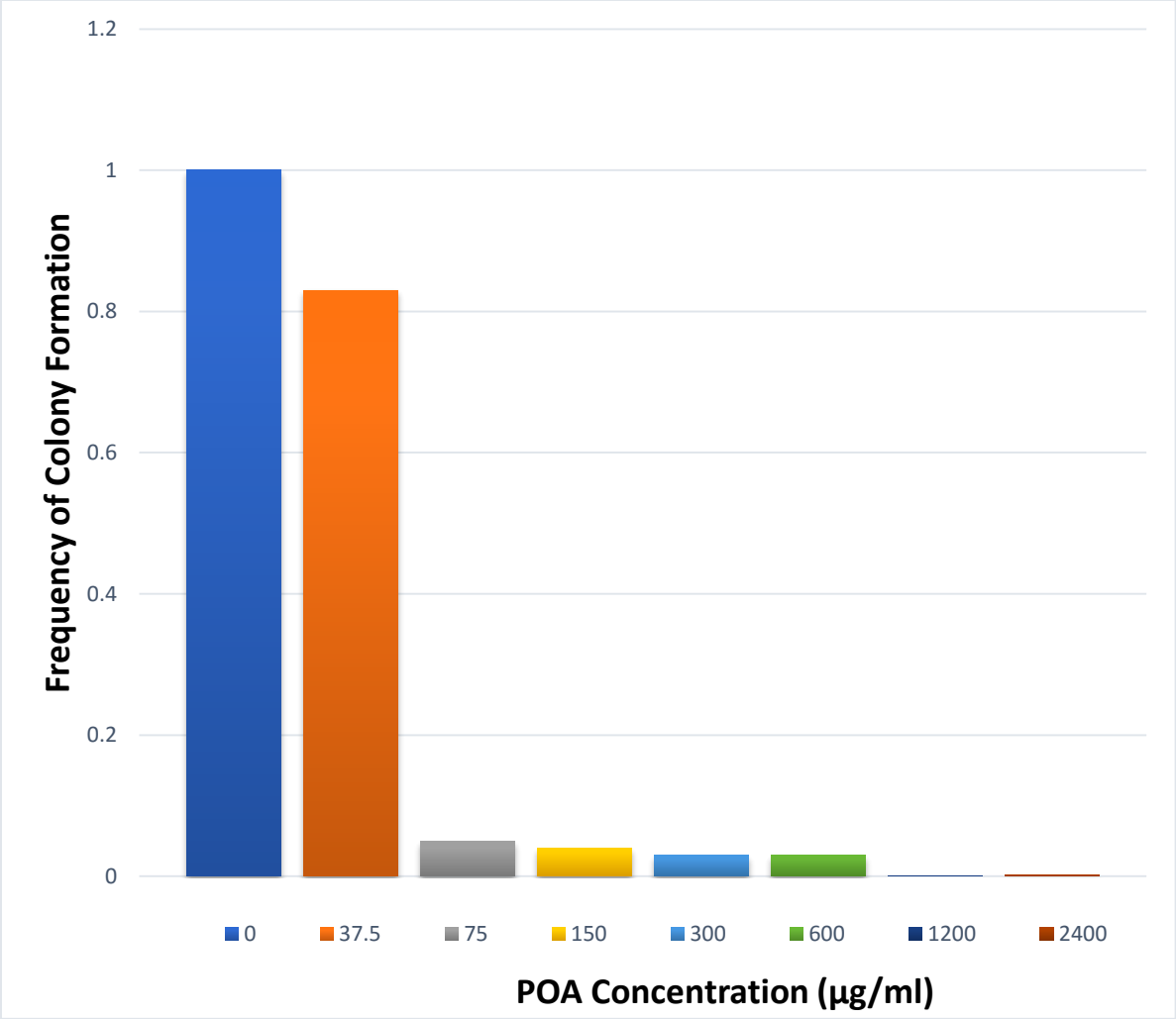

Figure 4.1: Phage infection potentiates POA action in BCG
Exponentially growing BCG was mutagenized with a phage carrying a mariner transposon, after which the mutagenized bacilli were plated on 7H10 agar plates containing POA concentrations of (0, 37.5, 75, 150, 300, 600, 1200 and 2400) µg/ml, and incubated for 14 days.

4.2 Isolation of POA resistant mutants

A total of 80 colonies were randomly selected from all the plates and subsequently grown in liquid medium. All the 6 colonies which were isolated on plates containing 2400 µg/ml did not grow in liquid medium. To determine if these transposon mutants were resistant to POA, their growth was assessed in standard liquid medium containing 200 µg/ml POA, which is the POA MIC_{90} for BCG at pH 6.8. A no drug control plate was also set up. Resistance was defined as strains showing a growth (OD_{600}) ratio of greater than 0.5 when exposed to POA compared to growth in the absence of POA. A total of 12 transposon mutants were resistant to POA as compared to the no drug control, and these resistant mutants were isolated from across all the POA plates except 150 µg/ml plate (Figure 4.2A). In addition, the MIC_{90} on agar medium (pH 5.8) was also determined for each mutant. MIC_{90} was defined as the concentration of POA that inhibits 90% of growth relative to the no drug control. The isolates displayed varying degrees of resistance to POA compared to the mutants isolated from the no drug control. The resistance ranged from 2 to 4-fold. Out of the 74 isolates, 12 were susceptible to the agar POA MIC_{90} (pH 5.8) of 200 µg/ml and 59 were susceptible to 400 µg/ml POA. These mutants were isolated from across all the POA plates. In addition, 3 mutants were resistant to the 200 µg/ml and 400 µg/ml POA and had an MIC of 800 µg/ml. These mutants were isolated from plates containing 150 µg/ml, 300 µg/ml and 600 µg/ml POA (Figure 4.2B).

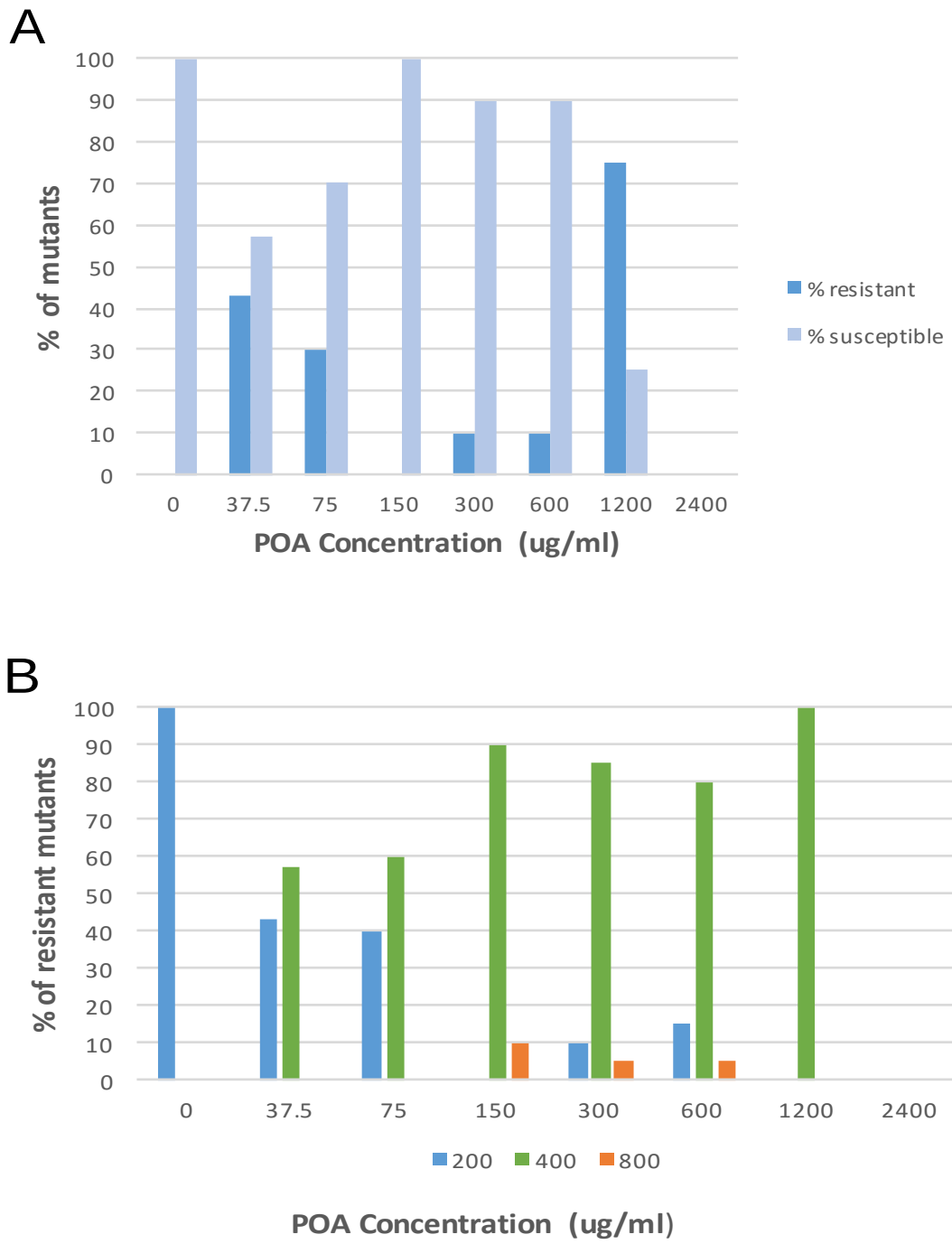

Figure 4.2: Isolation of POA resistant mutants
A) The susceptibility of selected transposon mutants to 200 µg/ml POA was tested after 21 days incubation in 7H9 + OADC +glycerol + tyloxapol at pH 6.8. **B)** The plate POA MIC for the selected transposon mutants was determined by growing them on 7H10 agar containing different POA concentrations at pH 5.8 after 21 days of incubation.

4.3 Analysis of POA Resistant Mutants

Four POA resistant mutants were randomly selected for follow up analysis. After POA susceptibility testing, a 2-fold resistance to POA on agar medium was observed in all four mutants. However, only 2 mutants had a 2-fold resistance to POA in liquid medium. The other 2 had the same susceptibility in liquid medium as compared to the wild type strain (Table 4.1). To identify the transposon insertion site of these mutants, genomic DNA was further extracted from these isolates and subsequently digested with *BssHII*, ligated, and used to transform *E. coli* DH5 λ pir. Plasmid DNA was purified after which the transposon junction was sequenced. Unique transposon insertion sites were identified comprising of two mutations in genes whose function have not been previously characterized. One mutation was seen in an intergenic region and the other seen in a gene that is suspected to be involved in triacylglycerol synthesis. Confirming the specificity of the resistance to POA, no difference in isoniazid (INH) susceptibility was found in the mutants compared to the wild type strain (Table 4.1).

Table 4.1 Phenotypic characterization of POA resistant mutations

Strain	Liquid (pH 6.8)		Agar (pH 5.8)	Function
	POA MIC_{90} (µg/ml)	INH MIC_{90} (ng/ml)	POA MIC_{90} (µg/ml)	
M. bovis BCG	200	60	200	
M. bovis BCG *Mb3814*::Tn	200	60	400	Hypothetical protein
M. bovis BCG *lps-pe26*::Tn	400	60	400	Intergenic region between LPPS and PE26
M. bovis BCG *Mb3284c*::Tn	400	60	400	Hypothetical protein
M. bovis BCG *Mb3509c*::Tn	200	60	400	May be involved in synthesis of triacylglycerol

MIC_{90} is the minimum concentration of drug that inhibits 90% of growth relative to the no drug control over 14 days of incubation. INH - Isoniazid

4.4 Testing of Synergy between PZA and H_2O_2

To test if PZA synergizes with H_2O_2 to kill *M. tuberculosis*, FIC experiments using 72 hours PZA pretreatment followed by H_2O_2 exposure were conducted in H37*Ra*. FICI is a measure of the degree of synergy between two compounds with synergy being defined as an FICI ≤ 0.5 from the experiment, PZA and H_2O_2 were synergistic against H37*Ra*, with an FICI of 0.0625 (Figure 4.3A). Given that the PZA conversion is strictly required for drug efficacy, we hypothesized that POA rather than PZA was directly involved in synergy with H_2O_2. The *M. bovis* attenuated vaccine strain BCG was used to examine the requirement for POA for synergy with H_2O_2. Like all *M. bovis* strains, BCG is naturally resistant to PZA due to a loss of function mutation in *pncA*, which encodes the nicotinamidase responsible for converting PZA to POA. Ectopic expression of *pncA* in BCG permits POA conversion promoting PZA susceptibility in this strain. As such, FIC experiments were carried out in wild type BCG and BCG-*pncA* to examine the requirement for POA conversion for synergy with H_2O_2. Similar to H37*Ra*, PZA synergized with H_2O_2 against BCG-*pncA* strain (FICI =0.3125) (Figure 4.3B). On the other hand, pre-incubation of wild type BCG with PZA did not alter susceptibility of the bacilli to H_2O_2, indicating that, POA conversion is required for synergy with H_2O_2 (Figure4.3C).

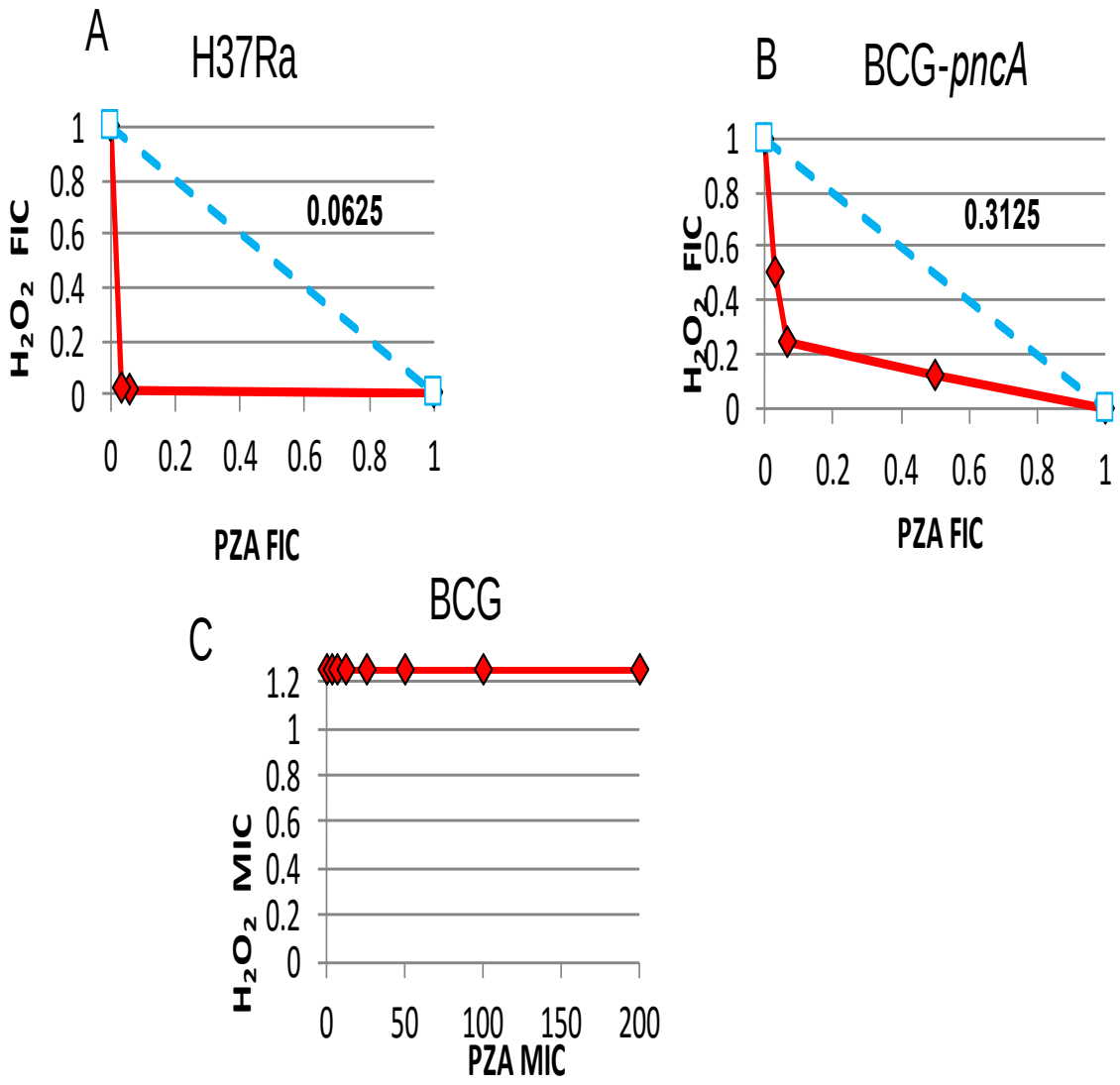

Figure 4.3: PZA treatment synergizes with H_2O_2 through a POA mediated mechanism

FIC plots were generated from the treatment of **A)** H37*Ra* and **B)** BCG-*pncA* with PZA 72 hours prior to being challenged with H_2O_2 in 7H9 + ADS +glycerol + tyloxapol at pH 5.8. **C)** MIC plot was generated from the treatment of BCG with PZA, 72 hours prior to being challenged with H_2O_2 in 7H9 + ADS +glycerol + tyloxapol at pH 5.8. Plots are representatives of three independent experiments and blue line represents the line of additivity.

4.5 *In silico* Construction of Allelic Exchange Substrate (AES) for *aceE* Deletion

Transposon mutagenesis identified mutations in *aceE* as a POA resistance conferring mutation. To further understand if *aceE* modulates PZA susceptibility, we set out to delete *aceE* in BCG and H37Ra using specialized transduction method of allelic exchange. The *in silico* AES for *aceE* deletion was constructed by Gibson assembly using NEBuilder assembly tool from New England Biolabs. Figure 4.4 below shows the output after the building of the construct. The total size of the construct is a 6988bp Baughn lab p0004S plasmid which has its hygromycin (*hygR*) and *sacB* cassette flanked by 850bp and 851bp upstream and downstream sequences of the *aceE* respectively. The assembly consists of a four-piece ligation of the pieces upstream, downstream, insert and backbone. The hygromycin (*hygR*) and *sacB* cassette represented as insert is 3673bp. The remaining sequence of the plasmid is 1614bp and designated as backbone. The program automatically generates primers for each piece of the assembly construct. The primer sequences for each piece contain uppercase nucleotides which are the forward and reverse primers for each assembly piece. In addition, it also contains lowercase nucleotides which serve as overlapping sequences for the assembly. The program also generates annealing temperatures for each primer (Figure 4.4).

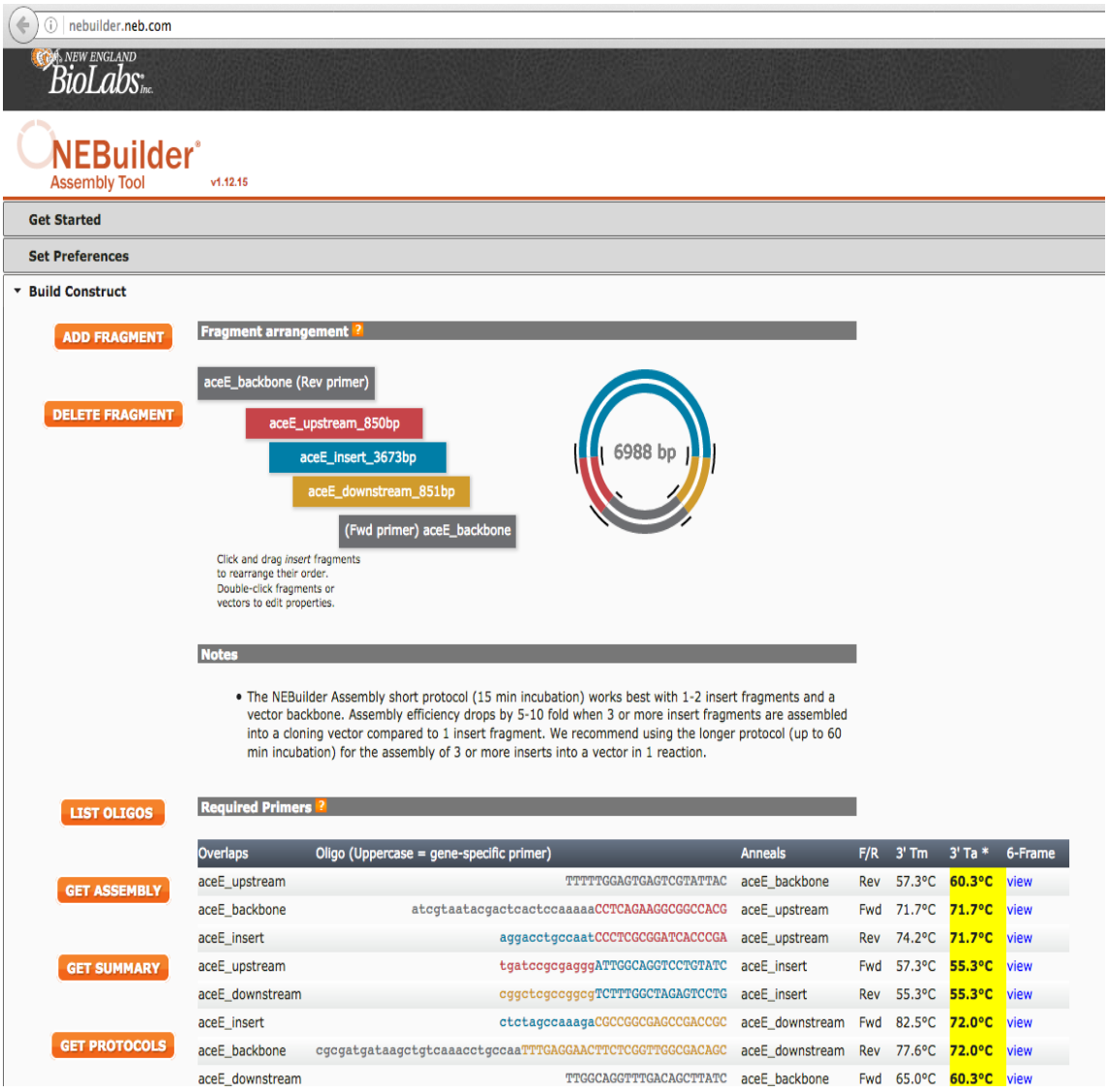

Figure 4.4: *In silico* design of allelic exchange substrate (AES) for *aceE* deletion
The AES for *aceE* deletion was constructed by Gibson assembly using NEBuilder assembly tool.

4.6 PCR Amplification of Gibson Assembly Pieces

The primers generated from NEBuilder assembly tool was used to amplify 850bp and 851bp upstream and downstream sequences of the *aceE* respectively from H37*Ra* genomic. Also, 1614bp and 3673bp plasmid backbone and insert fragments (hygromycin (*hygR*) and *sacB* cassette) respectively were amplified from p0004S plasmid (Figure 4.5).

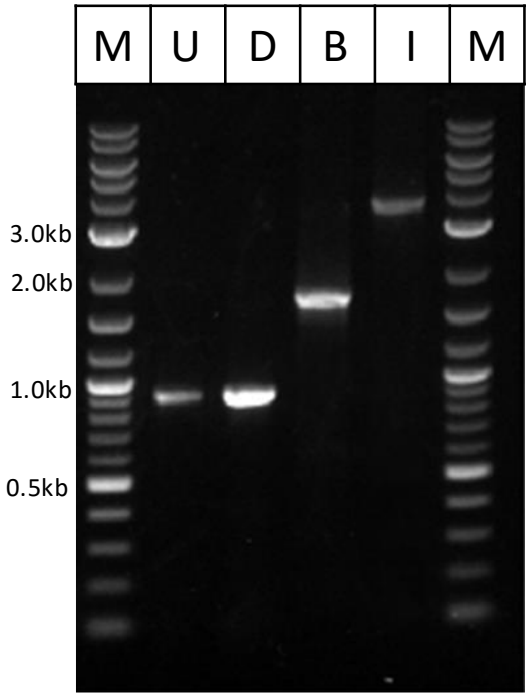

Figure 4.5: PCR amplification of Gibson assembly pieces
M-Molecular marker, U-Upstream, D-Downstream, B-Backbone, I-Insert
The Gibson assembly pieces were amplified from H37*Ra* genomic DNA and p0004S plasmid DNA using specific primers.

4.7 Restriction Digest to Confirm Correct Allelic Exchange Substrate

Verified PCR amplicons for the assembly pieces were purified after which they were assembled by a four-piece ligation reaction. The assembly reaction was transformed into DH5 α *E. coli* and subjected to selection on hygromycin plates. Hygromycin resistant colonies were screened by extracting plasmid DNA and running on 1% agarose gel after restriction digest with *XhoI* and *HpaI* to verify correct AES. The confirmed strains were sequenced verified, after which the sequences were compared to the *in silico* AES. Figure 4.6A shows *XhoI* restriction digest for 5 candidate plasmids. The expected band sizes for the correct AES is 822bp and 6166bp, and from the gel, only sample 3 gave the expected band pattern. Figure 4.6B shows *HpaI* restriction digest for the same plasmids, serving as a second confirmation of the correct AES. The expected band size is 6968bp. From the gel, plasmids 1, 2, 3 and 4 looked potentially positive. Control band of restriction digest of p0004S was not observed for both restriction digests, possibly due to low or degraded DNA. Sample 3 was selected and sequenced confirmed.

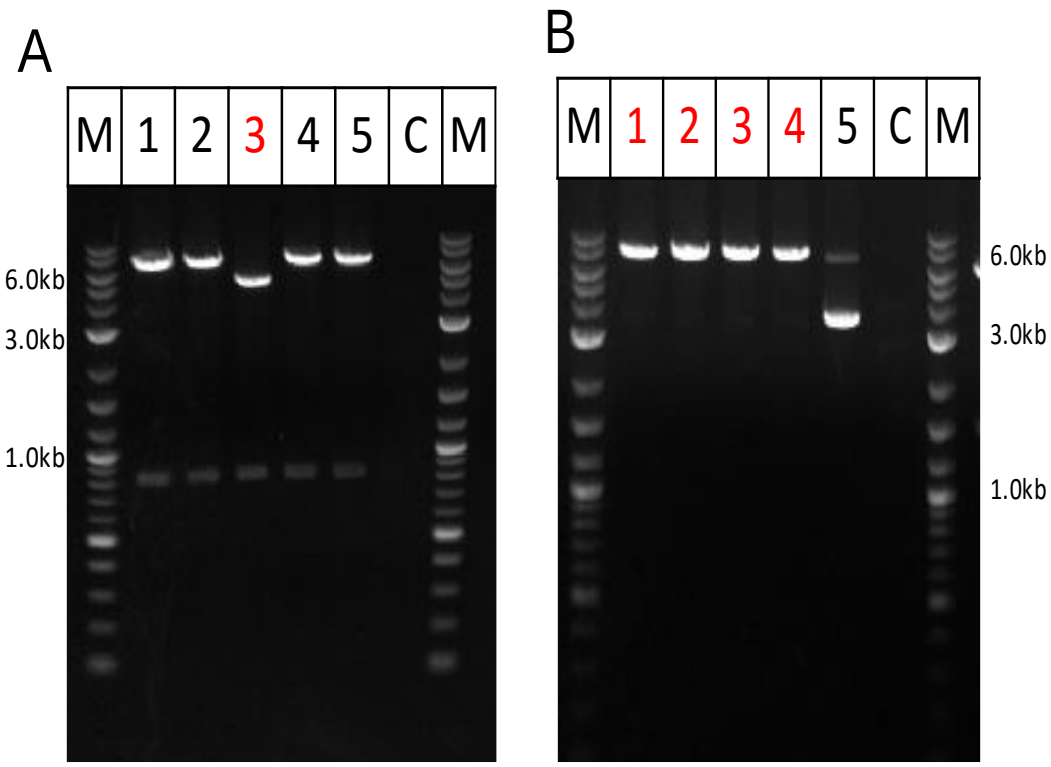

Figure 4.6: Restriction digest to confirm correct allelic exchange substrate
M- Molecular marker (2-log DNA ladder), 1-5 - Selected colonies, C- Control (p0004S). DNA of candidate plasmids obtained after Gibson assembly and *E coli* transformation was digested with **A)** *XhoI* and **B)** *HpaI* to verify correct AES.

4.8 Confirmation of Phasmid

To generate a phasmid which will be further used to prepare a deletion phage, confirmed AES and phasmid phAE159 were both digested with *PacI* and then ligated. The ligation product was packaged *in vitro* using a MaxPlax bacteriophage lambda packaging extract, and the resulting phage was used to transduce *E. coli* HB10 and subjected to selection on hygromycin plates. Hygromycin resistant colonies were subsequently screened for candidate phasmids by DNA extraction and *PacI* digestion. Expected band sizes for correct phasmid is a two-band pattern consisting of ~50kb for phae159 and 6988bp for AES. From Fig 4.7, phasmids 1, 2, 4 and 6 were positive.

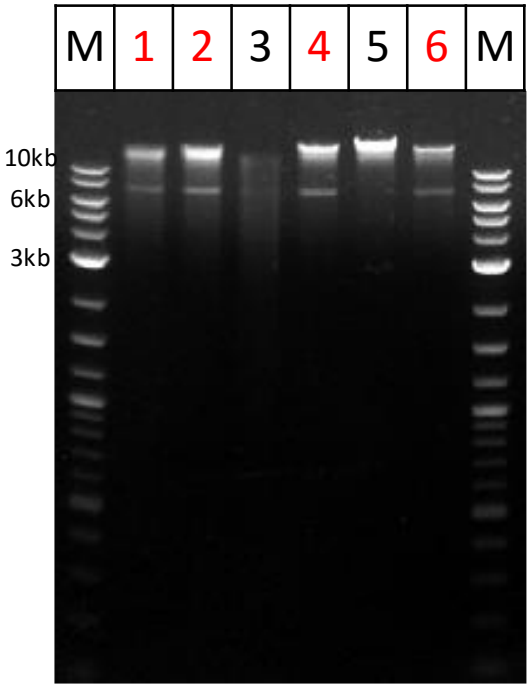

Figure 4.7: *PacI* digestion of phasmids
M- Molecular marker (2-log DNA ladder), 1-6 - Selected colonies
DNA from candidate phasmids obtained after *in vitro* packaging and *E. coli* transformation was digested with *PacI* to verify correct phasmid.

4.9 Preparation of *aceE* Deletion Phage

Confirmed phasmid was electroporated into *M. smegmatis* mc^2155 cells for mycobacteriophage propagation. The transformed cells were added to 3ml noble agar and subsequently plated on supplemented 7H10 agar medium and incubated at 30^oC for 3 days. Phage plaques were cored out into mycobacteriophage buffer to recover phage. The resulting phage was then propagated in *M. smegmatis* mc^2155 until a phage titer of 10^{10} pfu/ml was attained. Phage plaques were obtained during phage propagation (Figure 4.8A) and the titer was determined (Figure 4.8B) as 8.4 x 10^{10} pfu/ml. Subsequently, high titer phage was used to transduce *M. bovis* BCG and attenuated *M. tuberculosis* H37*Ra*.

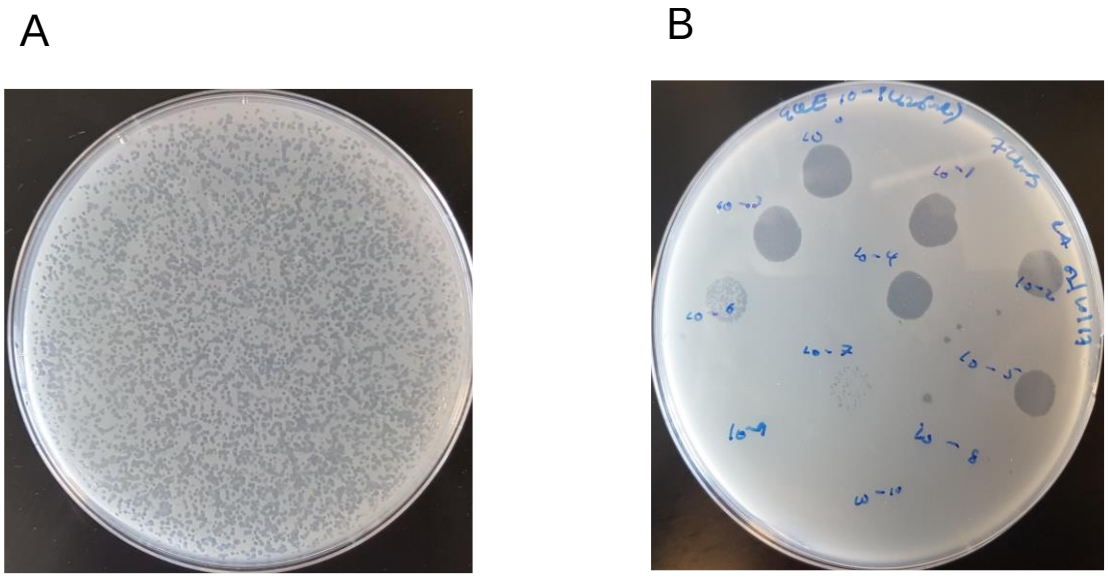

Phage plaques after propagation **Determination of phage titer**

Figure 4.8: Preparation of *aceE* deletion phage
Confirmed phasmids were electroporated into *M. smegmatis* for phage propagation. The resulting phage was taken through several propagation steps until a high titer phage was obtained.

4.10 Construction of *pckA* Overexpression Strain

Transposon mutagenesis also identified mutation in *pckA* as a POA resistance conferring mutation. To further evaluate if overexpression of *pckA* increases susceptibility to POA, it was over-expressed from a constitutive mycobacterial promoter using the replicating plasmid pUMN002 which contains a kanamycin selectable marker. *pckA* was amplified from BCG genomic DNA by PCR with primers containing *HindIII* and *NheI* restriction sites at the 5' and 3' ends respectively. An 1821bp positive *pckA* band was observed (Figure 4.9A). As negative control, plasmid pUMN002 was used as a template, and as expected, no band was observed. The resulting PCR product and plasmid pUMN002 were taken through a double restriction digest with *HindIII* and *NheI* resulting in a 4600bp pUMN002 band and 1821pb *pckA* band (Figure 4.9B). The digested products were ligated and then used to transform DH5 α *E. coli* and selected on kanamycin plates. Plasmid DNA was purified from 6 candidates and then subjected to *HindIII* and *NheI* double digest to confirm correct plasmid. All the plasmids were potentially positive due to the presence of expected pUMN002 and *pckA* band sizes of 4600bp and 1821bp respectively (Figure 4.9C). Also, as negative control, pUMN002 was digested and a single band of 4600bp was observed. Potentially positive plasmids were sequenced confirmed. Sequence confirmed plasmids were then electroporated into electrocompetent BCG and H37*Ra* cells and selected on kanamycin plates after 14 days' incubation. Plasmid DNA from the resulting colonies were taken through colony PCR to verify the presence of the 635bp kanamycin cassette. From Figure 4.9D, all candidate plasmids including the positive control showed the presence of the 635bp expected band size.

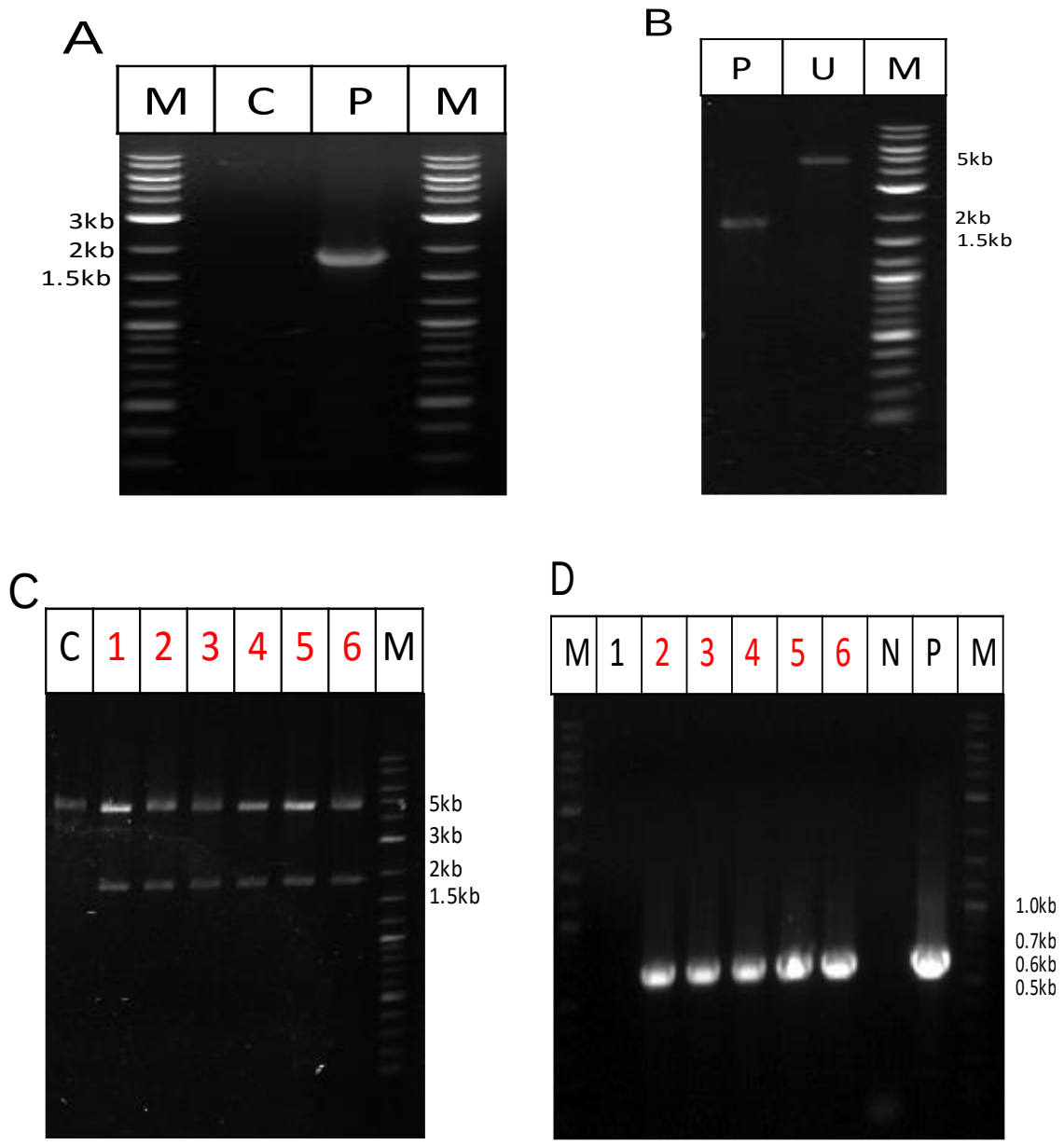

Figure 4.9: Construction of *pckA* overexpression strains

M- Molecular marker (2-log DNA ladder), **A)** C- Negative control using p0004S as a template, P- amplified *pckA*. **B)** P- digested *pckA*, U- digested pUMN002. **C)** 1-6 – restriction digest of potential plasmid candidates, C–control (restriction digest of pUMN002). **D)** 1-3 are candidate plasmids from BCG, 4-6 are candidate plasmids from H37*Ra*, N- negative control (H37*Ra* as PCR template), P- positive control (pUMN002 as PCR template).

pckA was amplified from BCG genomic DNA using primers containing *HindIII* and *NheI* restriction sites. The PCR product as well as plasmid pUMN002 was digested with *HindIII* and *NheI*, ligated and transformed into *E. coli*. Correct plasmid DNA was electroporated into BCG and H37Ra after digestion with *HindIII* and *NheI*. The resulting strains were screened for the presence of kanamycin cassette and confirmation of correct construct.

4.11 Determination of *pckA* Expression Level by Quantitative Reverse Transcription PCR (qRT-PCR)

To evaluate if *pckA* was being over-expressed, the expression level was determined by qRT-PCR. RNA was extracted from exponential phase cultures of both wildtype and mutant *M. bovis* BCG and H37Ra, followed by qRT-PCR. The level of *pckA* expression was normalized to *SigA*. There was no change in the expression levels of *pckA* in the mutant strain in relation to the wildtype strain for both *M. bovis* BCG and H37*Ra* (Figure 4.10).

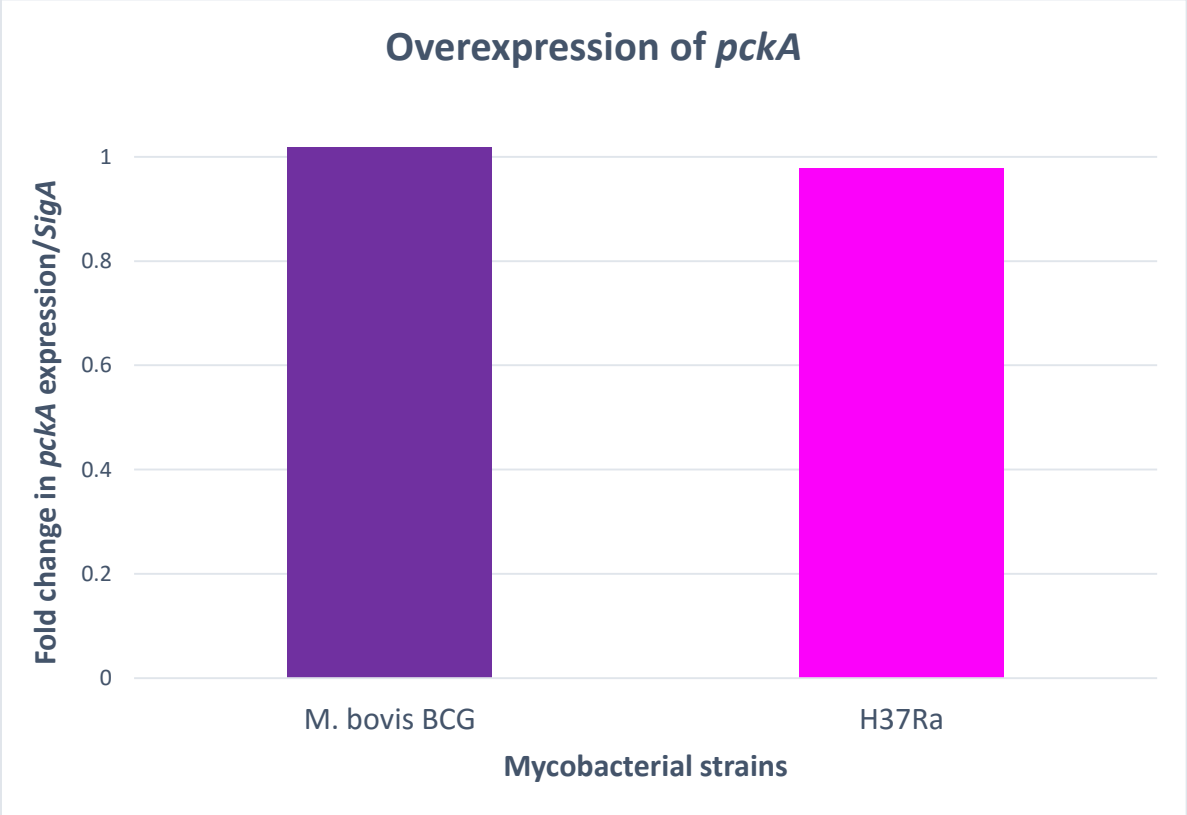

Figure 4.10: Determination of *pckA* expression levels in BCG and H37Ra.
RNA was extracted from mid exponential phase wild type and *pckA* overexpression BCG and H37*Ra* strains. The expression of *pckA* was quantified by qRT-PCR and its expression level was normalized to *Sig A* level.

4.12 POA Susceptibility Testing

To further evaluate if overexpression of *pckA* increases susceptibility to POA, antimicrobial susceptibility testing was conducted in both mutant and wild type BCG and H37*Ra* at pH 6.8 and pH 5.8. There was a 2-fold reduction in the MIC_{90} of the mutant BCG as compared to the wildtype at both testing conditions. However, there was no difference observed in the POA MIC_{90} of H37Ra mutant and wild type strains at both conditions (Figure 4.11).

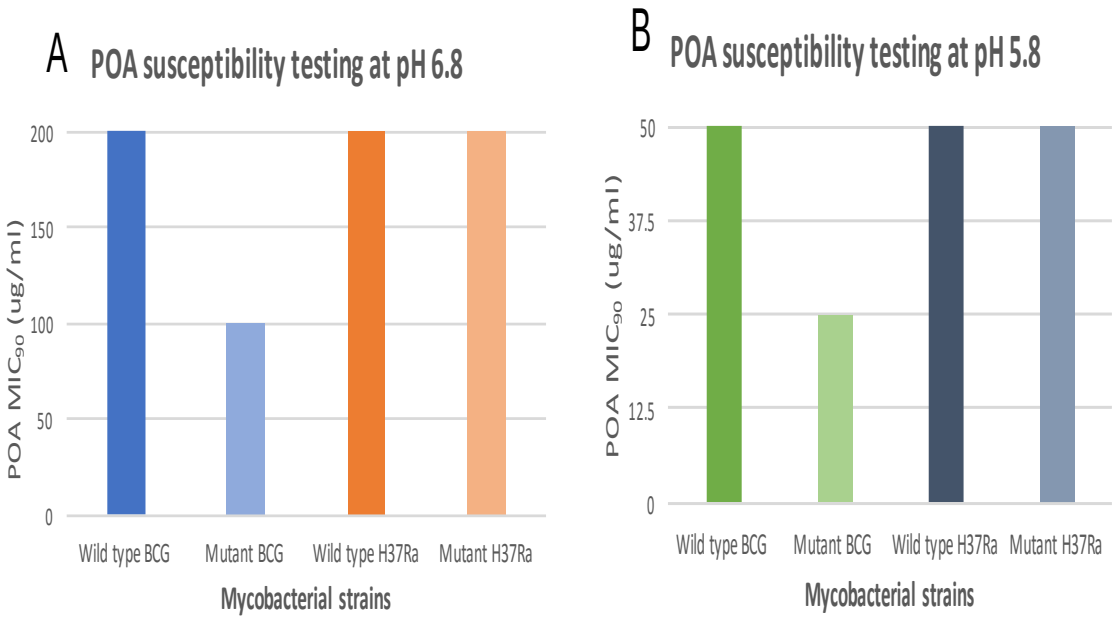

Figure 4.11: POA susceptibility testing in mutant and wild type BCG and H37*Ra*

MIC_{90} is the minimum concentration of drug that inhibits 90% of growth relative to the no drug control after 14 days of incubation

CHAPTER FIVE

5.0 DISCUSSION

5.1 Transposon Mutagenesis and Isolation of POA Resistant Mutants

Approximately one third of PZA clinical resistant isolates are resistant through unidentified mechanisms. Therefore, to gain a better understanding of *M tuberculosis* resistance to PZA, we sought to identify POA resistance conferring mutations in *M. tuberculosis* by insertional transposon mutagenesis, using *M. bovis* BCG as a model system. Transposon mutagenesis is a great tool that has been used to identify several genetic elements that regulate specific phenotypes. It has been used to identify the functions of several genes in cancer (Chen *et al.,* 2017), malaria (Ikadai *et al.,* 2013) and other infectious diseases (Chiang *et al*., 1999).

A *Himar1* mariner based transposon was used to mutagenize BCG. The transposon mutants were plated on sub-inhibitory concentrations of POA to ascertain if phage infection potentiates POA action in BCG as observed in H37Rv (Unpublished data). From the data, it was observed that phage infection sensitizes BCG to POA up to about 32 fold (Figure 4.1). There was however an observed disparity between the resistance pattern of the transposon mutants in liquid and agar media (Figure 4.2). This reason for the differences in susceptibility on different media is not clearly known. Nonetheless, this disparity has been observed with other antimicrobial drugs (Rylander *et al.,* 1979).

While the mechanism of action of PZA remains undefined, *in vitro* susceptibility to the drug requires concurrent exposure to stresses such as: acidic pH (McDermott & Tompsett, 1954), hypoxia (Wade & Zhang, 2004), nutrient limitation (Peterson *et al.,* 2015), and heat

shock (Coleman *et al.*, 2011). However, phage potentiation of POA action has never been reported in literature. The mechanistic role these stresses play in potentiating PZA action has not been elucidated although evidence indicates that it is not through altered *pncA* expression (Peterson *et al., 2015).* Recently, our lab identified mutation in the gene for the mycobacteria stress response sigma factor *sigE* in POA resistant transposon mutants. A follow-up study with a *sigE* knockout mutant showed increased resistance to PZA. Complementation of the gene restored PZA susceptibility back to wild type levels (Unpublished results). SigE is known to respond to cell surface stresses such as oxidative damage, SDS treatment, peptidoglycan damage, heat shock and low pH, besides modulating other genes and transcription factors in *M. tuberculosis* (Manganelli *et al.,* 2001). Similarly, the above stresses are the same stresses required for potentiating PZA action. From this data, it is possible that phage potentiation of POA action that was observed, acts by induction of SigE regulon, which subsequently sensitizes the *M. tuberculosis* bacilli to POA. Further work is being done in our lab to solve the elusive mechanism of PZA action through the newly observed connections between SigE induction, CoA level modulation, and PZA susceptibility.

Unlike some strains which are resistant to several drugs, the POA resistant transposon mutants analyzed from this study showed resistance specifically to POA, but not isoniazid (INH), one of the drugs in the treatment regimen (Table 4.1). This shows that, the resistance conferring mutations are specific to POA. Next generation sequences of the remaining transposon mutants will generate novel mutations that can further be analyzed to understand the mechanism for these resistance conferring mutations.

Currently, WHO has no standardized culture-based drug sensitivity testing for PZA due to the need for an acidified medium for susceptibility. The medium acidification generates variable results, and prevents the growth of some bacterial species (Chang *et al.*, 2011). An excessively large inocula is also required for the test, and this mostly reduces PZA activity (Zhang *et al.*, 2002), leading to false resistance. As such, several studies are trying to employ phage based methods for drug susceptibility testing (Park *et al.*, 2003). Phage based assays promise to be more cost effective and rapid (Eltringham *et al.*, 1999). Thus, the phage potentiation observed in this study opens a great and new avenue for phage based PZA susceptibility testing. This method has the advantage of eliminating the conditions which poses a problem to PZA susceptibility.

5.2 Synergy between Host Induced Oxidative Stress and PZA Action

Due to the host environment *M. tuberculosis* finds itself, as well as the conditional susceptibility of PZA *in vivo*, we hypothesized that host induced oxidative burst synergizes with PZA to kill *M. tuberculosis.* We tested this hypothesis by performing checkerboard assays to test synergy between PZA and exogenously provided H_2O_2. Results from our study confirmed our hypothesis and shows that PZA synergizes with H_2O_2 (Figure 4.3A and 4.3B). Similar results were seen in the virulent H37Rv strain of *M. tuberculosis* (data not shown). Given that PZA conversion is strictly required for drug efficacy, we hypothesized that POA rather than PZA was directly involved in synergy with H_2O_2. The *M. bovis* attenuated vaccine strain BCG was used to examine the requirement for POA for synergy with H_2O_2. Like all *M. bovis* strains, BCG is naturally resistant to PZA due to a loss of function mutation in *pncA*, which encodes the nicotinamidase responsible for

converting PZA to POA (Scorpio & Zhang, 1996) .

From our study, we observed that, pre-incubation of wild type BCG with PZA did not alter susceptibility of the bacilli to H_2O_2, indicating that, POA conversion is required for synergy with H_2O_2 (Figure4.3C). These *in vitro* results were also confirmed in an *ex vivo* study with macrophages when it was observed that, addition of the antioxidant N-acetyl cysteine (NAC) abolished PZA activity in *M. tuberculosis* infected IFNγ activated macrophages (data not shown).

A possible explanation to this observed synergy is that, oxidative stress potentiates POA action by oxidizing thiol active CoA thereby reducing its availability, resulting in the inability of the bacterium to conduct its essential metabolic activities and thus, resulting in its killing. In addition, POA treatment likely acts by sensitizing the *M. tuberculosis* bacilli to killing by host oxidative stress, since from the checkerboard assays, sub-inhibitory levels of H_2O_2 were capable of bactericidal activity against *M. tuberculosis* when combined with PZA. Because H_2O_2 is produced by early host responses against *M. tuberculosis* within the phagosome, from our results, a hardy immune system would therefore be required to potentiate POA activity. A dysfunctional or weak host induced oxidative burst would render POA less effective due to the absence of an exogenous H_2O_2 source. This is likely the basis for reduced PZA activity observed in immune-compromised hosts (Almeida *et al.,* 2014) as well as in inactivated resting macrophages. Furthermore, the dependence on exogenous reactive oxygen species (ROS) may also explain the conditional susceptibility of PZA *in vitro*.

The search for improved anti-mycobacterial therapies is on the rise, and this study proposes

a new route for potentiating PZA activity. To enhance PZA action, compounds that would boost phagosomal oxidative stress can be developed. Also, targeting the ability of *M. tuberculosis* to cope with oxidative stress is expected to enhance PZA treatment.

5.3 Construction of *aceE* Knockout Mutant by Specialized Transduction

PZA has been suggested to disrupt bacterial central carbon metabolism. Recent studies have also shown that PZA acts by depletion of coenzyme A (CoA) levels in *M. tuberculosis* (Gopal *et al.,* 2016 and Rosen *et al.,* 2017). Using transposon mutagenesis, our laboratory also identified mutations in the *pckA* and *aceE* in PZA resistant isolates (Unpublished data). Since these two genes are involved in central carbon metabolism by inducing acetyl-CoA production and thereby reducing free CoA, we hypothesized that, maintaining a higher steady state level of CoA through disruption of *aceE* or *pckA* genes in *Mycobacterium tuberculosis* is responsible for the PZA resistance phenotypes of these strains. To confirm our hypothesis, we set out to delete *aceE* in BCG and H37*Ra* using a slightly modified version of specialized transduction method of allelic exchange and gene deletion in mycobacteria (Bardarov *et al.*, 2002 and Jain *et al.*, 2014).

From the study, the deletion phage was generated and subsequently used to transduce BCG and H37*Ra*, to generate the deletion mutant. After the transduction, about 15 potential colonies were obtained on the hygromycin selection plates for BCG. However, these colonies did not grow when cultured in standard liquid medium. Conversely, no colonies were observed on H37*Ra* plates. Pyruvate dehydrogenase complex, of which *aceE* is an important component, is required in the conversion of pyruvate to acetyl-CoA which is

then used in the citric acid cycle. This complex serves as a major metabolic junction that links the glycolysis metabolic pathway to the citric acid cycle. Considering the importance of this complex and how essential *aceE* is to the growth of *M. tuberculosis*, the growth medium was supplemented with 0.5% glutamic acid serving as another entry point into the TCA cycle. However, this supplementation was not sufficient to promote the growth of the mutant strains even after 6 weeks of culture. From the transposon screen carried out in our lab, *aceE* mutants had a growth defect, consistent with the essentiality of the gene in the metabolism of *M. tuberculosis.* Until date, no study has successfully constructed a knockout mutant of *aceE* in *M. tuberculosis* possibly because it is essential for its metabolism and survival. Nonetheless, *aceE* has been deleted in *Salmonella enterica* (Pang *et al.,* 2011).

One possible way to study the function of a likely essential gene in *M. tuberculosis* is by employing a gene silencing route. A unique dual-control (DUC) switch method that combines repression of transcription and controlled proteolysis to silence gene activities in *M. tuberculosis* was developed recently (Kim *et al.,* 2013). This method of gene silencing identified proteins that *M. tuberculosis* requires for growth *in vitro* and during infections. Thus, this method can be employed.

5.4 Overexpression of *pckA* in BCG and H37*Ra*

Transposon mutagenesis in our laboratory also identified mutation in *pckA* as a POA resistance conferring mutation. Therefore, to evaluate if overexpression of *pckA* increases susceptibility to POA, it was over-expressed from a constitutive mycobacterial promoter

using the replicating plasmid pUMN002. After the overexpression strain was constructed, the expression level of *pckA* was compared to that of the wild type strain by qRT-PCR. The results did not show increased overexpression of *pckA* in both BCG and H37*Ra* mutant strains (Figure 4.10). On the contrary, the mutant BCG strain showed a two-fold increased susceptibility to POA compared to wild type strains at both pH 6.8 and pH 5.8. No increased susceptibility to PZA was observed in the H37*Ra* mutant strain at both conditions (Figure 4.11).

The disparity between mRNA levels and observed phenotype could have been because of the following reasons. It is possible that the primer for the qRT-PCR was not designed properly, as such, was not able to accurately measure the expression of the mRNA. New set of primers would therefore have to be designed to rectify this. Also, in prokaryotes, translation and transcription are parallel processes, since prokaryotic ribosomes initiate translation of the mRNA transcript while DNA is still being transcribed. The rate of translation depends on the rate at which a ribosome is recruited to the ribosome binding site (RBS) and the rate at which a recruited ribosome can efficiently initiate translation. These factors affecting the rate of translation are affected by the RBS sequence. The plasmid pUMN002 has a very strong RBS, as such, it is possible that the strength of the RBS can cause increased protein translation even with low transcript levels. Although mRNA expression levels are generally used as a substitute for estimating functional differences that occur at the protein level, efforts to compare the abundance of protein with the expression levels of mRNA have had variable success rates (Gygi *et al.*, 1999 and Chen *et al.*, 2002). A western blot can therefore be employed to confirm if the protein is being overexpressed in the mutant strain in comparison to the wild type. Another way to further

confirm overexpression of *pckA* is to conduct enzymatic assays to determine if the activity of phosphoenolpyruvate carboxykinase is increased in the overexpression strain as opposed to the wild type.

Finally, the phenotypic differences observed in BCG and H37*Ra* is not surprising (Figure 4.11). Our laboratory has observed several discrepancies in using H37*Ra* in recombinant molecular biology work. For example, conducting transposon mutagenesis as well as gene deletion in H37*Ra* has been highly unsuccessful and the reason for this is currently not known.

CHAPTER SIX

6.0 CONCLUSIONS AND RECOMMENDATIONS

6.1 Conclusions

In conclusion, it has been observed that phage infection potentiates POA action in BCG possibly through induction of SigE regulon. We were also able to generate a POA resistant mutant library as well as novel POA resistance conferring mutations. These mutations are likely to predict the identity of the remaining clinical PZA resistance strains, potentially increasing the capability to genetically determine PZA susceptibility in the clinic.

Finally, the working model from this study predicts that, PZA synergizes with host induced oxidative stress to decreases the availability of thiol active CoA levels in *M. tuberculosis*, resulting in its killing. This model attempts to explain the contrasting *in vivo* and *in vitro* conditional susceptibilities of PZA.

This study could guide future drug discovery efforts in creating compounds that can maintain the same mechanism of action as PZA but is able to circumvent the established resistance mechanisms.

6.2 Recommendations

1. The importance of host induced reactive oxygen species for PZA action needs to be further tested *in vivo*. This can be achieved by administering PZA to *M. tuberculosis* infected mutant mice incapable of generating host induced oxidative burst, for example NADPH oxidase mutant mice. To confirm our model, PZA action is expected to be abolished in these mice. Furthermore, from our

experiments, it is not clear if all the phagosomal derived stresses are required for inducing PZA susceptibility. Additional experiments are therefore required to determine if PZA activity is dependent on other sources of stress generated within phagocytes.

2. The POA resistant transposon mutant library generated needs to be further analyzed to understand the mechanisms for the resistance conferring mutations.

REFERENCES

Ahmad, S. (2011). Pathogenesis, immunology, and diagnosis of latent Mycobacterium tuberculosis infection. *Clinical and Developmental Immunology*, *2011*, 17.

Ahmad, Z., Tyagi, S., Minkowski, A., Almeida, D., Nuermberger, E. L., Peck, K. M., ... & Grosset, J. H. (2012). Activity of 5-chloro-pyrazinamide in mice infected with *Mycobacterium tuberculosis* or *Mycobacterium bovis*. *The Indian journal of medical research*, *136*(5), 808.

Almeida, D. V., Tyagi, S., Li, S., Wallengren, K., Pym, A. S., Ammerman, N. C., Bishai, W. R. & Grosset, J. H. (2014). Revisiting Anti-tuberculosis Activity of Pyrazinamide in Mice. *Mycobacterial. Diseases, Tuberculosis and Leprosy*, *4*, 145.

American Thoracic Society and Centers for Disease Control and Prevention. (2000). Diagnostic standards and classification of tuberculosis in adults and children. American Journal of Respiratory and Critical Care Medicine, 161(4.1), 1376-1395.

Amo-Adjei, J. & Awusabo-Asare, K. (2013). Reflections on tuberculosis diagnosis and treatment outcomes in Ghana, *Arch Public Health*, 71, 22.

Bardarov, S., Bardarov Jr, S., Pavelka Jr, M. S., Sambandamurthy, V., Larsen, M., Tufariello, J., ... & Jacobs Jr, W. R. (2002). Specialized transduction: an efficient method for generating marked and unmarked targeted gene disruptions in *Mycobacterium tuberculosis, M. bovis BCG* and *M. smegmatis*. *Microbiology*, *148*(10), 3007-3017.

Batra, V. (2011). Overview of tuberculosis. Pediatric Tuberculosis. http://tinyurl.com/3zm76h2 (Accessed 7 September 2011)

Baughn, A. D., & Rhee, K. Y. (2014). Metabolomics of Central Carbon Metabolism in *Mycobacterium tuberculosis. Microbiology Spectrum*, *2*(3), MGM2-0026-2013.

Begley, T. P., Kinsland, C., Mehl, R. A., Osterman, A. & Dorrestein, P. (2001). The biosynthesis of nicotinamide adenine dinucleotides in bacteria. *Vitamins and*

Hormones , 61, 103.

Bernstein, J., Lott, W. A., Steinberg, B. A., & Yale, H. L. (1952). Chemotherapy of experimental tuberculosis. V. Isonicotinic acid hydrazide (nydrazid) and related compounds. *American Review of Tuberculosis and Pulmonary Diseases, 65*(4), 357-364.

Betts, J. C., Lukey, P. T., Robb, L. C., McAdam, R. A., & Duncan, K. (2002). Evaluation of a nutrient starvation model of *Mycobacterium tuberculosis* persistence by gene and protein expression profiling. *Molecular microbiology, 43*(3), 717-731.

Boehme, C.C., Nabeta, P. & Hillemann, D. (2010). Rapid molecular detection of tuberculosis and rifampin resistance. *New England Journal of Medicine*, 363(11), 1005–15.

Boshoff, H. I., Myers, T. G., Copp, B. R., McNeil, M. R., Wilson, M. A., & Barry, C. E. (2004). The transcriptional responses of *Mycobacterium tuberculosis* to inhibitors of metabolism novel insights into drug mechanisms of action. *Journal of Biological Chemistry*, *279*(38), 40174-40184.

Boshoff, H. I., Xu, X., Tahlan, K., Dowd, C. S., Pethe, K., Camacho, L. R., ... & Williams, K. J. (2008). Biosynthesis and recycling of nicotinamide cofactors in *Mycobacterium tuberculosis* an essential role for nad in nonreplicating bacilli. *Journal of Biological Chemistry*, *283*(28), 19329-19341.

Campbell, E. A., & Korzheva, N. (2001). Structural Mechanism for Rifampicin Inhibition of Bacterial RNA Polymerase. *Cell, 104*, 901–912.

Cardona, P. J. (2009). A dynamic reinfection hypothesis of latent tuberculosis infection. *Infection*, *37*(2), 80–86.

CDC. (2005). Guidelines for preventing the transmission of *Mycobacterium tuberculosis* in health-care settings. *MMWR, 54* (No. RR-17). www.cdc.gov/mmwr/preview/mmwrhtml/rr5417a1.htm?s_cid=rr5417a1_e

Cepheid International (2011). Two-hour detection of MTB and resistance to rifampicin, www.cepheidinternational.com

Chang, K. C., Yew, W. W., & Zhang, Y. (2011). Pyrazinamide susceptibility testing in *Mycobacterium tuberculosis*: a systematic review with meta-analyses. *Antimicrobial agents and chemotherapy*, *55*(10), 4499-4505.

Chen, G., Gharib, T. G., Huang, C. C., Taylor, J. M., Misek, D. E., Kardia, S. L., ... & Beer, D. G. (2002). Discordant protein and mRNA expression in lung adenocarcinomas. *Molecular & cellular proteomics*, *1*(4), 304-313.

Chen, L., Jenjaroenpun, P., Pillai, A. M. C., Ivshina, A. V., Ow, G. S., Efthimios, M., ... & Ward, J. M. (2017). Transposon insertional mutagenesis in mice identifies human breast cancer susceptibility genes and signatures for stratification. *Proceedings of the National Academy of Sciences*, *114*(11), E2215-E2224.

Chiang, C. W., Carter, N., Sullivan, W. J., Donald, R. G., Roos, D. S., Naguib, F. N., ... & Wilson, C. M. (1999). The Adenosine Transporter of *Toxoplasma gondii*; identification by insertional mutagenesis, cloning, and recombinant expression. *Journal of Biological Chemistry*, *274*(49), 35255-35261.

Ciccarelli, L., Connell, S. R., Enderle, M., Mills, D. J., Vonck, J., & Grininger, M. (2013). Structure and conformational variability of the *Mycobacterium tuberculosis* fatty acid synthase multienzyme complex. *Structure*, *21*(7), 1251-1257.

Coleman, D., Waddell, S. J., & Mitchison, D. A. (2010). Effects of low incubation temperatures on the bactericidal activity of anti-tuberculosis drugs. *Journal of Antimicrobial Chemotherapy*, *66*(1), 146-150.

Connolly, L. E., Edelstein, P. H., & Ramakrishnan, L. (2007). Why Is Long-Term Therapy Required to Cure Tuberculosis? *PLoS Med 4* (3): e120.

Cynamon, M. H., Speirs, R. J., & Welch, J. T. (1998). In vitro antimycobacterial activity of 5-chloropyrazinamide. *Antimicrobial agents and chemotherapy*, *42*(2), 462-463.

Darby, C. M., Ingólfsson, H. I., Jiang, X., Shen, C., Sun, M., Zhao, N., ... & Anderson, O. S. (2013). Whole cell screen for inhibitors of pH homeostasis in *Mycobacterium tuberculosis*. *PloS one*, *8*(7), e68942.

Dessau, F., Yeager, R., Burger, F. & Williams, J. (1952). Pyrazinamide (aldinamide) in experimental tuberculosis of the guinea pig. *The American review of tuberculosis*, *65*, 519–522.

Dheda, K., Booth, H., & Huggett, J. F., (2005). Lung remodeling in pulmonary tuberculosis. *Journal of Infectious Diseases*, *192*, 1201-1210.

Dillon, N. A., Peterson, N. D., Feaga, H. A., Keiler, K. C., & Baughn, A. D. (2017). Anti-tubercular Activity of Pyrazinamide is Independent of trans-Translation and RpsA. *Scientific Reports*, *7*.

Dillon, N. A., Peterson, N. D., Rosen, B. C., & Baughn, A. D. (2014). Pantothenate and pantetheine antagonize the antitubercular activity of pyrazinamide. *Antimicrobial agents and chemotherapy*, *58*(12), 7258-7263.

Dormandy, T. (1999). The white death. London: Hambledon Press.

Eltringham, I. J., Wilson, S. M., & Drobniewski, F. A. (1999). Evaluation of a bacteriophage-based assay (phage amplified biologically assay) as a rapid screen for resistance to isoniazid, ethambutol, streptomycin, pyrazinamide, and ciprofloxacin among clinical isolates of *Mycobacterium tuberculosis. Journal of clinical microbiology*, *37*(11), 3528-3532.

Escalante, P. (2009).In the clinic. Tuberculosis. *Annals of Internal Medicine*, *150*(11), 61–614.

Fang, F. C. (2004). Antimicrobial reactive oxygen and nitrogen species: concepts and controversies. *Nature Reviews Microbiology*, *2*, 820–832.

Fisher, J. F. & Mobashery, S. (2010). Enzymology of Bacterial Resistance. Comprehensive Natural Products II. Volume 8: Enzymes and Enzyme Mechanisms. Elsevier, 443–201.

Foster, J. W., & Moat, A. G. (1980) Nicotinamide adenine dinucleotide biosynthesis and pyridine nucleotide cycle metabolism in microbial systems. *Microbiology Review, 44*(1), 83–105.

Ghana Health Service (GHS) (2015). Tuberculosis Control Programme report.

Gopal, P., Yee, M., Sarathy, J., Low, J. L., Sarathy, J. P., Kaya, F., Dartois, … Dick, T. (2016). Pyrazinamide Resistance Is Caused by Two Distinct Mechanisms: Prevention of Coenzyme A Depletion and Loss of Virulence Factor Synthesis. *ACS Infectious Diseases, 2*(9), 616-626.

Gygi, S. P., Rochon, Y., Franza, B. R., & Aebersold, R. (1999). Correlation between protein and mRNA abundance in yeast. *Molecular and cellular biology*, *19*(3), 1720-1730.

Hu, Y., Coates, A. R., & Mitchison, D. A. (2006). Sterilising action of pyrazinamide in models of dormant and rifampicin-tolerant *Mycobacterium tuberculosis*. *The International Journal of Tuberculosis and Lung Disease, 10*(3), 317-322.

Huang, Q., Chen, Z. F., Li, Y. Y., Zhang, Y., Ren, Y., Fu, Z., & Xu, S. Q. (2007). Nutrient-starved incubation conditions enhance pyrazinamide activity against *Mycobacterium tuberculosis. Chemotherapy*, *53*(5), 338-343.

Huant, E. (1945). Note sur l'action de tres fortes doses d'amide nicotinique dans les lesion bacillaires. *Gazette Hopitau*, *118*, 259-60.

Ikadai, H., Saliba, K. S., Kanzok, S. M., McLean, K. J., Tanaka, T. Q., Cao, J., ... & Jacobs-Lorena, M. (2013). Transposon mutagenesis identifies genes essential for *Plasmodium falciparum* gametocytogenesis. *Proceedings of the National Academy of Sciences, 110*(18), E1676-E1684.

Ilina, E. N., Shitikov, E. A., Ikryannikova, L. N., Alekseev, D. G., Kamashev, D. E., Malakhova, M. V., ... & Smirnova, T. G. (2013). Comparative genomic analysis of *Mycobacterium tuberculosis* drug resistant strains from Russia. *PloS one*, *8*(2), e56577.

Iseman, M. D. (2002). Tuberculosis therapy: past, present and future. *The European Respiratory Journal*, *20*, 87–94.

Jain, P., Hsu, T., Arai, M., Biermann, K., Thaler, D. S., Nguyen, A., ... & Larsen, M. H. (2014). Specialized transduction designed for precise high-throughput unmarked deletions in *Mycobacterium tuberculosis. MBio*, *5*(3), e01245-14.

Joint Tuberculosis Committee of the British Thoracic Society. (2000). Control and prevention of tuberculosis in the United Kingdom: code of practice. *Thorax*, 887-901.

Juréen, P., Werngren, J., Toro, J. C., & Hoffner, S. (2008). Pyrazinamide resistance and pncA gene mutations in *Mycobacterium tuberculosis*. *Antimicrobial agents and chemotherapy*, *52*(5), 1852-1854.

Kalokhe, A. S., Shafiq, M., Lee, J. C., Ray, S. M., Wang, Y. F., Metchock, B., ... & Nguyen, M. L. T. (2013). Multidrug-resistant tuberculosis drug susceptibility and molecular diagnostic testing: a review of the literature. *The American journal of the medical sciences*, *345*(2), 143.

Keane, J., Balcewicz-Sablinska, M. K., Remold, H. G., Chupp, G. L., Meek, B. B., Fenton, M. J., & Kornfeld, H. (1997). "Infection by *Mycobacterium tuberculosis* promotes human alveolar macrophage apoptosis". *Infections Immunology, 65 (1), 298–304.*

Kim, J. H., O'Brien, K. M., Sharma, R., Boshoff, H. I., Rehren, G., Chakraborty, S., ... & Barry, C. E. (2013). A genetic strategy to identify targets for the development of drugs that prevent bacterial persistence. *Proceedings of the National Academy of Sciences*, *110*(47), 19095-19100.

Klemens, S. P., Sharpe, C. A., & Cynamon, M. H. (1996). Activity of pyrazinamide in a murine model against *Mycobacterium tuberculosis* isolates with various levels of in vitro susceptibility. *Antimicrobial agents and chemotherapy*, *40*(1), 14-16.

Köser, C. U., Comas, I., Feuerriegel, S., Niemann, S., Gagneux, S., & Peacock, S. J. (2014). Genetic diversity within *Mycobacterium tuberculosis complex* impacts on the accuracy of genotypic pyrazinamide drug-susceptibility assay. *Tuberculosis*, *94*(4), 451-453.

Konstantinos, A. (2010). Testing for tuberculosis. *Australian Prescriber*, *33*(1), 12–18.

Kushner, S., Dalalian, H., Sanjurjo, J. L., Bach Jr, F. L., Safir, S. R., Smith Jr, V. K., & Williams, J. H. (1952). Experimental chemotherapy of tuberculosis. II. The synthesis of pyrazinamides and related compounds1. *Journal of the American Chemical Society*, *74*(14), 3617-3621.

Lachâtre, M., Rioux, C., Le Dû, D., Fréchet-Jachym, M., Veziris, N., Bouvet, E., & Yazdanpanah, Y. (2016). *The Lancet*, *16*, 294.

Lawn, S. D. (2000). Tuberculosis in Ghana: social stigma and compliance with treatment. *The International Journal of Tuberculosis and Lung Disease*, 4, 1190–1191.

Lawn, S. D. & Zumla, A. I. (2011). "Tuberculosis". *Lancet*, *378*, 57–72.

Lorenz, M., & Fink, G. (2002). Life and Death in a Macrophage: Role of the Glyoxylate Cycle in Virulence. *Eukaryotic Cell*, *1*(5), 657–662.

Louw, G. E., Warren, R. M., Donald, P. R., Murray, M. B., Bosman, M., Van Helden, P. D., ... & Victor, T. C. (2006). Frequency and implications of pyrazinamide resistance in managing previously treated tuberculosis patients. *The International Journal of Tuberculosis and Lung Disease*, *10*(7), 802-807.

Malone, L., Schurr, A., Lindh, H., McKenzie, D., Kiser, J. S., & Williams, J. H. (1952). The Effect of Pyrazinamide (Aldinamide) on Experimental Tuberculosis in Mice. *American Review of Tuberculosis and Pulmonary Diseases*, *65*(5), 511-518.

Manganelli, R., Voskuil, M. I., Schoolnik, G. K., & Smith, I. (2001). The *Mycobacterium tuberculosis* ECF sigma factor σE: role in global gene expression and survival in macrophages. *Molecular microbiology*, *41*(2), 423-437.

Maslov D. A., Shur K. V., Bekker O. B., Zakharevich N. V., Zaichikova M. V., Klimina K. M., Smirnova T. G.,… Danilenko V. N. (2015). Draft genome sequences of two pyrazinamide-resistant clinical isolates, *Mycobacterium tuberculosis* 13-4152 and 13-2459. *Genome Announcements*, 3(4), e00758-15.

Mayer, B. & Hemmens, B. (1997). Biosynthesis and action of nitric oxide in mammalian cells. *Trends in Biochemical Sciences, 22*, 477–481.

McCune, R.M. Jr., & Tompsett, R. (1956). Fate of *Mycobacterium tuberculosis* in mouse tissues as determined by the microbial enumeration technique. I. The persistence of drug-susceptible tubercle bacilli in the tissues despite prolonged antimicrobial therapy. *Journal of Experimental Medicine, 104*, 737–762.

McCune, R. M., Tompsett, R., & McDermott, W. (1956). The fate *of Mycobacterium tuberculosis* in mouse tissues as determined by the microbial enumeration technique. *Journal of Experimental Medicine*, *104*(5), 763-802.

McDermott, W., & Tompsett, R. (1954). Activation of pyrazinamide and nicotinamide in acidic environments *in vitro*. *The American review of tuberculosis*, *70*, 748–754.

McKinney, J. D., zu Bentrup, K. H., Munoz-Elias, E. J., Miczak, A., Chen, B., Chan, W. T., Swenson, D., … Russell, D. G. (2000). Persistence of *Mycobacterium tuberculosis* in macrophages and mice requires the glyoxylate shunt enzyme isocitrate lyase. *Nature, 406*(6797), 735-738.

Metcalfe, J. Z, Everett, C. K., Steingart, K. R., Cattamanchi, A., Huang, L., Hopewell, P. C., & Pai, M. (2011). "Interferon-γ release assays for active pulmonary tuberculosis diagnosis in adults in low- and middle-income countries: systematic review and meta-analysis". *Journal of Infectious Diseases, 204*, 1120–1129.

Migliori, G. B., De Iaco, G., Besozzi, G., Centis, R., & Cirillo, D. M. (2007). First tuberculosis cases in Italy resistant to all tested drugs. *Eurosurveillance, 12*(20).

Milburn, H. (2007). Key issues in the diagnosis and management of tuberculosis. *Journal of Royal Society of Medicine, 100*(3), 134–141.

Minakami, R., & Sumimotoa, H. (2006). Phagocytosis-coupled activation of the superoxide-producing phagocyte oxidase, a member of the NADPH oxidase (nox) family. *International. Journal of Hematology, 84*, 193–198.

Mitchison, D. A. (1985). The action of antituberculosis drugs in short-course chemotherapy. *Tubercle*, *66*(3), 219-225.

Müller, B., Chihota, V. N., Pillay, M., Klopper, M., Streicher, E. M., Coetzee, G. & Warren, R. M. (2013). Programmatically Selected Multidrug-Resistant Strains Drive the Emergence of Extensively Drug-Resistant Tuberculosis in South Africa. *PLoS ONE*, 8(8), e70919.

National Institute for Health and Clinical Excellence. (2006). Tuberculosis:clinical diagnosis and management of tuberculosis, and measures for its prevention and control. London: NICE. Available at: www.nice.org.uk/page. aspx?o=CG033.

National Tuberculosis Programme (NTP) Ghana (2014). Report on World Tuberculosis Day Commemoration.

Nicod, L. P. (2007). Immunology of tuberculosis. *Swiss Medical Weekly, 137*(25-26):357-362.

Ormerod, L. P., & Horsfield, N. (1987). Short-course antituberculous chemotherapy for pulmonary and pleural disease: 5 years' experience in clinical practice. *British Journal of Diseases of the Chest, 81*, 268–271.

Osei-Wusu, S., Amo Omari, M., Asante-Poku, A., Darko Otchere, I., Asare, P., Forson, A., … Yeboah-Manu, D. (2018). Second-line anti-tuberculosis drug resistance

testing in Ghana identifies the first extensively drug-resistant tuberculosis case. *Infection and Drug Resistance*, *11*, 239–246.

Pang, E., Tien-Lin, C., Selvaraj, M., Chang, J., & Kwang, J. (2011). Deletion of the aceE gene (encoding a component of pyruvate dehydrogenase) attenuates *Salmonella enterica serovar Enteritidis*. *FEMS Immunology & Medical Microbiology*, *63*(1), 108-118.

Park, D. J., Drobniewski, F. A., Meyer, A., & Wilson, S. M. (2003). Use of a phage-based assay for phenotypic detection of mycobacteria directly from sputum. *Journal of clinical microbiology*, *41*(2), 680-688.

Peterson, N. D., Rosen, B. C, Dillon, N. A., & Baughn, A. D., (2015). Uncoupling environmental pH and intrabacterial acidification from pyrazinamide susceptibility in *Mycobacterium tuberculosis*. *Antimicrobial Agents and Chemotherapy* , *59*(12), 7320-7326.

Porth, C. M. (2002). Alterations in respiratory function: respiratory tract infections, neoplasms, and childhood disorders. In: Porth, C. M., Kunert, M. P. Pathophysiology: Concepts of Altered Health States. Philadelphia, PA: Lippincott Williams & Wilkins, pp 615-619.

Rosen, B. C., Dillon, N. A., Peterson, N. D., Minato, Y., & Baughn, A. D. (2017). Long-Chain Fatty Acyl Coenzyme A Ligase FadD2 Mediates Intrinsic Pyrazinamide Resistance in *Mycobacterium tuberculosis. Antimicrobial agents and chemotherapy*, *61*(2), e02130-16.

Rylander, M., Brorson, J. E., Johnsson, J., & Norrby, R. (1979). Comparison between agar and broth minimum inhibitory concentrations of cefamandole, Cefoxitin, and cefuroxime. *Antimicrobial agents and chemotherapy*, *15*(4), 572-579.

Sanwal, B. D. (1970). Allosteric Controls of Amphibolic Pathways in Bacteria. *Bacteriological Reviews*, *34*, 20-39.

Sassetti, C. M., Boyd, D. H., & Rubin, E. J. (2003). Genes required for mycobacterial growth defined by high density mutagenesis. *Molecular Microbiology*, *48*, 77–84.

Sassetti, C. M., & Rubin, E. J. (2003). Genetic requirements for mycobacterial survival during infection. *Proceedings of the National Academy of Sciences*, *100*, 12989–12994.

Saunder, B. M., & Britton, W. J. (2007). Lifeanddeathinthegranuloma: immunopathology of tuberculosis. *Immunology and Cell Biology, 85*(2), 103–111.

Schluger, N. W. (2005). The Pathogenesis of Tuberculosis the First One Hundred (and Twenty-Three) Years. *American Journal of Respiratory Cell Molecular Biology, 32*, 251–256.

Scorpio, A., Lindholm-Levy, P., Heifets, L., Gilman, R., Siddiqi, S., Cynamon, M., & Zhang, Y. (1997). Characterization of pncA mutations in pyrazinamide-resistant *Mycobacterium tuberculosis*. *Antimicrobial Agents and Chemotherap*y, *41*(3), 540-543.

Scorpio, A., Lindholm-Levy, P., Heifets, L., Gilman, R., Siddiqi, S., Cynamon, M., & Zhang, Y. (1997). Characterization of pncA mutations in pyrazinamide-resistant Mycobacterium tuberculosis. *Antimicrobial agents and chemotherapy*, *41*(3), 540-543.

Scorpio A. & Zhang Y. (1996). Mutations in pncA, a gene encoding pyrazinamidase/nicotinamidase, cause resistance to the antituberculous drug pyrazinamide in tubercle bacillus. *Nature Medicine*, *2*(6), 662–667.

Shi, W., Chen, J., Feng, J., Cui, P., Zhang, S., Weng, X., ... & Zhang, Y. (2014). Aspartate decarboxylase (PanD) as a new target of pyrazinamide in *Mycobacterium tuberculosis*. *Emerging microbes & infections*, *3*(8), e58.

Shi, S., & Ehrt, S. (2006). Dihydrolipoamide acyltransferase is critical for *Mycobacterium tuberculosis* pathogenesis. *Infection and immunity*, *74*(1), 56-63.

Shi, W., Zhang, X., Jiang, X., Yuan, H., Lee, J. S., Barry, C. E., ... & Zhang, Y. (2011). Pyrazinamide inhibits trans-translation in *Mycobacterium tuberculosis*. *Science*, *333*(6049), 1630-1632.

Solotorovsky, M., Gregory, F. J., Ironson, E. J., Bugie, E. J., O'Niell, R. C. & Pfister, K. (1952). Pyrazinoic acid amide-an agent active against experimental murine tuberculosis. *Experimental Biology and Medicine, 79,* 563–565.

Somner, A. & Angel, J. (1981). A controlled trial of six months chemotherapy in pulmonary tuberculosis: first report: results during chemotherapy. *British Journal of Diseases of the Chest, 75,* 141–153.

Speirs, R. J., Welch, J. T., & Cynamon, M. H. (1995). Activity of n-propyl pyrazinoate against pyrazinamide-resistant *Mycobacterium tuberculosis*: investigations into mechanism of action of and mechanism of resistance to pyrazinamide. *Antimicrobial agents and chemotherapy, 39*(6), 1269-1271.

Steele, M. A., & Des Prez, R. M. (1988). The role of pyrazinamide in tuberculosis chemotherapy. *Chest*, *94*(4), 845-850.

Tabshis, M., & Weed Jr, W. A. (1953). Lack of significant in vitro sensitivity of *Mycobacterium tuberculosis* to pyrazinamide on three different solid media. *American Review of Tuberculosis and Pulmonary Diseases*, *67*(3), 391-395.

Takeda, K. & Akira, S. (2005). Toll-like receptors in innate immunity. *International Immunology, 17*(1), 1–14.

Tan, Y., Hu, Z., Zhang, T., Cai, X., Kuang, H., Liu, Y., ... & Zhao, Y. (2014). Role of pncA and rpsA gene sequencing in detection of pyrazinamide resistance in *Mycobacterium tuberculosis* isolates from southern China. *Journal of clinical microbiology*, *52*(1), 291-297.

Tanaka, A., Atomi, H., Ueda, M., Hikida, M., Hishida, T., & Teranishi, Y. (1990). "Peroxisomal isocitrate lyase of the n-alkane-assimilating yeast Candida tropicalis:

gene analysis and characterization". *Journal of Biochemistry*, *107*(2), 262–266Telenti, A., Philipp, W. J, Sreevatsan, S., Bernasconi, C., Stockbauer, K. E., Wieles, B., Musser, J. M., & Jacobs, W. R. Jr. (1997). The emb operon, a gene cluster of *Mycobacterium tuberculosis* involved in resistance to ethambutol. *Nature Medicine, 3*, 567–70.

Telles, M. A., & Kritski, A., (2007). Biosafety and hospital control In: Palomino, J. C., Leão, S. C., Ritacco, V. (eds) Tuberculosis 2007: From Basic Science to Patient Care http://tinyurl. com/3wbkq78 (Accessed 7 September 2011)

Tiemersma, E. W., Van der Werf, M. J., Borgdorff, M. W., Williams, B. G. & Nagelkerke, N. J. D. (2011). Natural history of tuberculosis: Duration and fatality of untreated pulmonary tuberculosis in HIV negative patients: A systematic review. *PLoS One*, *6*(4), e17601.

Timmins, G. S., & Deretic, V. (2006). Mechanism of action of isoniazid. *Molecular Biology*, *62* (5), 1220-1227.

Tummon, R. (1975). Growth inhibition of *Mycobacterium tuberculosis* by oleate in acidified medium. *Medical laboratory technology*, *32*(3), 229-232.

Turgut, M., Akhaddar, A., Turgut, A. T., Garg, R. T. (2017). Tuberculosis of the Central Nervous System: Pathogenesis, Imaging and Management, Switzerland, Springer publishing.

Udwadia, Z. F., Amale, R. A., Ajbani, K. K. & Rodrigues, C. (2011). Totally Drug-Resistant Tuberculosis in India. *Clinical Infectious Diseases, 54*, 579–581.

van Crevel, R., Ottenhoff, T. H. M., & van der Meer, J. W. M. (2002). Innate immunity to *Mycobacterium tuberculosis*. *Clinical Microbiology Review, 15*, 294-309.

Vandal, O. H., Pierini, L. M., Schnappinger, D., Nathan, C. F., & Ehrt, S. (2008). A membrane protein preserves intrabacterial pH in intraphagosomal *Mycobacterium tuberculosis*. *Nature medicine, 14*(8), 849-854.

Velayati, A. A., Masjedi, M. R., Farnia, P., Tabarsi, P., Ghanavi, J., Ziazarifi, A. H., & Hoffner, S. E. (2009). Emergence of new forms of totally drug-resistant tuberculosis bacilli: super extensively drug-resistant tuberculosis or totally drug- resistant strains in Iran. *Chest, 136*, 420–425.

Venugopal, A., Bryk, R., Shi, S., Rhee, K., Rath, P., Schnappinger, D., ... & Nathan, C. (2011). Virulence of *Mycobacterium tuberculosis* depends on lipoamide dehydrogenase, a member of three multienzyme complexes. *Cell host & microbe*, *9*(1), 21-31.

Wade, M. M., & Zhang, Y. (2004). Anaerobic incubation conditions enhance pyrazinamide activity against *Mycobacterium tuberculosis*. *Journal of medical microbiology*, *53*(8), 769-773.

Wani, S. R. L., (2013). Clinical manifestations of pulmonary and extra-pulmonary tuberculosis. *South Sudan Medical Journal, 6*(3), 52-56.

Wayne, L. G. (1974). Simple pyrazinamidase and urease tests for routine identification of mycobacteria. *American review of respiratory disease*, *109*(1), 147-151.

Whitfield, M. G., Soeters, H. M., Warren, R. M., York, T., Sampson, S. L., Streicher, E. M., ... & Van Rie, A. (2015). A global perspective on pyrazinamide resistance: systematic review and meta-analysis. *PloS one*, *10*(7), e0133869.

World Health Organization (2003).World Health Organization Stop TB Department. Treatment of tuberculosis: guidelines for national programmes, 3rd ed.. Geneva.

World Health Organization (2004). Weekly epidemiological record, *4* (79), 25–40.

World Health Organization. (2017). Global Tuberculosis report. World Health Organization, Geneva, Switzerland.

Yeager, R. L., Munroe, W. G. C. & Dessau, F. I. (1952). Pyrazinamide (aldinamide) in the treatment of pulmonary tuberculosis. *The American review of tuberculosis*, *65*, 523–

546.

Zhang, S., Chen, J., Shi, W., Liu, W., Zhang, W., & Zhang, Y. (2013). Mutations in panD encoding aspartate decarboxylase are associated with pyrazinamide resistance in *Mycobacterium tuberculosis*. *Emerging microbes & infections*, *2*(6), e34.

Zhang, Y., & Mitchison, D. (2003). The curious characteristics of pyrazinamide: a review. *The international journal of tuberculosis and lung disease*, *7*(1), 6-21.

Zhang, Y., Permar, S., & Sun, Z. (2002). Conditions that may affect the results of susceptibility testing of *Mycobacterium tuberculosis* to pyrazinamide. *Journal of medical microbiology*, *51*(1), 42-49.

Zhang, Y., Scorpio, A., Nikaido, H. & Sun, Z. (1999). Role of acid pH and deficient efflux of pyrazinoic acid in the unique susceptibility of *Mycobacterium tuberculosis* to pyrazinamide. *Journal of Bacteriology,* 181, 2044–2049.

Zhang, Y., & Yew, W. W. (2009). Mechanisms of drug resistance in *Mycobacterium tuberculosis* [State of the art series. Drug-resistant tuberculosis. Edited by CY. Chiang. Number 1 in the series]. *The International Journal of Tuberculosis and Lung Disease*, *13*(11), 1320-1330.

Zimhony, O., Cox, J. S., Welch, J. T., & Jacobs Jr, W. R. (2000). Pyrazinamide inhibits the eukaryotic-like fatty acid synthetase I (FASI) of *Mycobacterium tuberculosis*. *Nature medicine*, *6*(9), 1043.

Zuniga, J., Torres-Garcıa, D., Santos-Mendoza, T., Rodriguez-Reyna, T. S., Granados, J., & Yunis, E. J. (2012). Cellular and Humoral Mechanisms Involved in the Control of Tuberculosis. *Clinical and Developmental Immunology*, *18*

APPENDIX

Table A1: List of oligonucleotide primers used in this study

Name of primer	Sequence 5' to 3'
Kan_Rev_Seq	GCATCGCCTTCTATCGCCTTC
Kan_For	TATGACTGGGCACAACAGAC
Kan_Rev	AATATCACGGGTAGCCAACG
pckA_For	TTTTTTAAGCTTGCA GGA GAA TTC GAT GAC CTC AG
pckA_Rev	TTTTTTGCTAGCCTA ACC TAG GCG CTC CTT CAG
pT_For	CAT CCC GGC GTT GAT CTG TG
pT_Rev	TAA TCG CGG CCT CGA GCA AG
pckA_qrt_For	CGGGAGATCTGGAGCTACG
pckA_qrt_Rev	TAGCACTTCTTGCCCAGCA
sigA_For	TCAAACAGATCGGCAAGGT
sigA_Rev	CGCTAAGCTCGGTCATCAG
aceE_backbone_ fwd	TTGGCAGGTTTGACAGCTTATC
aceE_backbone_ rev	TTTTTGGAGTGAGTCGTATTAC
aceE_upstream_ fwd	atcgtaatacgactcactccaaaaaCCTCAGAAGGCGGCCACG
aceE_upstream_rev	aggacctgccaatCCCTCGCGGATCACCCGA
aceE_insert_fwd	tgatccgcgagggATTGGCAGGTCCTGTATC
aceE_insert_rev	cggctcgccggcgTCTTTGGCTAGAGTCCTG
aceE_downstream fwd	ctctagccaaagaCGCCGGCGAGCCGACCGC
aceE_downstream_ rev	cgcgatgataagctgtcaaacctgccaaTTTGAGGAACTTCTCGGTTGGC GACAGC